

# Theory of Heat Transport of Normal Liquid $^3\text{He}$ in Aerogel

J. A. Sauls

*Department of Physics & Astronomy, Northwestern University, Evanston, IL 60208*

Priya Sharma

*Department of Physics, Royal Holloway University of London, Egham, Surrey, TW20 0EX, UK*

(Dated: November 21, 2018)

The introduction of liquid  $^3\text{He}$  into silica aerogel provides us with a model system in which to study the effects of disorder on the properties of a strongly correlated Fermi liquid. The transport of heat, mass and spin exhibits cross-over behavior from a high temperature regime, where inelastic scattering dominates, to a low temperature regime dominated by elastic scattering off the aerogel. We report exact and approximate solutions to the Boltzmann-Landau transport equation for the thermal conductivity of liquid  $^3\text{He}$ , including elastic scattering of quasiparticles by the aerogel and inelastic quasiparticle collisions. These results provide quantitative predictions for the transport properties of liquid  $^3\text{He}$  in aerogel over a wide range of pressure, temperature and aerogel density. In particular, we obtain a scaling function,  $F(T/T_*)$ , for the normalized thermal conductivity,  $\kappa/\kappa_{el}$ , in terms of a reduced temperature,  $T/T_*$ , where  $T_*$  is a cross-over temperature defined by the elastic and inelastic collision rates. Theoretical results are compared with the available experimental data for the thermal conductivity.

PACS numbers: 67.10.-j, 67.10.Jn, 67.30.-n, 67.30.E-, 67.30.eh, 67.30.ej, 67.30.hm

Keywords: quantum fluids, liquid helium, aerogel, transport theory, diffusion, thermal conductivity

## I. INTRODUCTION

Aerogels are extremely low density solids formed as a rigid network of silica strands and clusters having a typical diameter of 30-50 Å and porosities ( $\rho$ ) above 99%.<sup>15</sup> They turn out to be an ideal system for studying the effects of quenched random disorder on the otherwise pure, ordered phases of liquid  $^3\text{He}$ . When impregnated with liquid  $^3\text{He}$ , the aerogel is found to have dramatic effects on the transport properties and the phase diagram of liquid  $^3\text{He}$ , although basic thermodynamic features characteristic of the Fermi liquid, such as the compressibility, magnetization and heat capacity, are essentially unchanged.<sup>18</sup> The low temperature transport of mass, heat and magnetization is substantially reduced.<sup>28,30,31</sup> In addition, the superfluid transition temperature as well as the superfluid order parameter are strongly suppressed relative to their bulk values.<sup>28,36</sup>

In this paper we consider the effects of scattering of  $^3\text{He}$  quasiparticles off a uniformly distributed random potential representing the aerogel structure, referred to as the “homogeneous scattering model” (HSM).<sup>38</sup> We obtain exact and approximate solutions to the Boltzmann-Landau transport equation for the thermal conductivity of liquid  $^3\text{He}$ , including both inelastic collisions between quasiparticles and elastic scattering of quasiparticles by the random potential. The chief inadequacy of the HSM is its neglect of the inhomogeneous void-structure of the aerogel, or more generally mesoscopic correlations that are observed in static structure factor, and to which the superfluid transition temperature is sensitive.<sup>27,34,38</sup> However, the transport properties are limited by the mean free path for quasiparticles propagating

ballistically within the aerogel, and hence are expected to be well accounted for in the framework of the HSM since the geometric *mfp* ( $\ell$ ) is typically much longer than the aerogel correlation length ( $\xi_a$ ), e.g.  $\ell/\xi_a \simeq 3$  for a 98% aerogel. Possible corrections to transport processes resulting from a small distribution of large voids or to fractal correlations on mesoscopic length scales  $\lesssim \xi_a$  within the aerogel are not included in the analysis presented in this work. However, the exact solution to the transport equation for the two-channel scattering model discussed in this paper should be of value in identifying observable corrections associated with correlated disorder or corrections to the two channel scattering theory.

Liquid  $^3\text{He}$  is a dense quantum liquid in which the interactions between Fermionic excitations (quasiparticles) are one to two orders of magnitude larger than the mean kinetic energy per particle. These interactions lead to strongly renormalized branches of Fermionic excitations, reflecting the correlated motion of many  $^3\text{He}$  atoms, and the emergence of Bosonic excitations. The Fermionic excitations bear resemblance to  $^3\text{He}$  atoms only in terms of their quantum numbers for spin ( $s = \pm 1/2$ ) and fermion number ( $e = \pm 1$ ). The Bosonic excitations come with and without spin and can be understood in terms of pairs of Fermionic excitations, e.g. the phonons of zero sound. Finally, the coupling between the Bosonic and Fermionic excitations leads to finite lifetimes for both types of excitations.<sup>4,21–23</sup>

Interactions between  $^3\text{He}$  quasiparticles enhance the collision rate for quasiparticles near the Fermi surface, leading to a significant reduction in the lifetime of a quasiparticle at the Fermi surface. However, Fermi statistics rescues the low-energy quasiparticles (as well as the Bosonic modes).<sup>40</sup> At low temperatures,  $T \ll E_f/k_B \approx 1\text{ K}$ , the number of exci-

tations is low,  $n_{\text{qp}} \approx (k_B T / E_f) n$ . Similarly, binary collision processes are confined to a small region of phase space near the Fermi surface,  $\Delta p \approx (k_B T / E_f) p_f$ . As a result the Pauli exclusion effect suppresses the quasiparticle collision rate,<sup>4</sup>

$$\frac{1}{\tau_{\text{in}}} = \frac{m^*{}^3}{4\pi^4 \hbar^6} \langle W \rangle (k_B T)^2 \sim T^2, \quad (1)$$

where  $m^*$  is the effective mass of a quasiparticle and  $\langle W \rangle$  is the square of the transition matrix element for binary collisions averaged over the Fermi surface.

Furthermore, since the density of excitations is low,  $n_{\text{qp}} \ll n$ , transport coefficients are given by formulae familiar from gas kinetic theory. In particular, the transport of heat is dominated by thermally excited quasiparticles with the thermal conductivity given by<sup>4</sup>

$$\kappa = \frac{1}{3} (\bar{c}_v v_f) (v_f \tau_\kappa), \quad (2)$$

where  $\bar{c}_v = \frac{2\pi^2}{3} N_f k_B^2 T$  is the low-temperature specific heat,  $N_f$  is the quasiparticle density of states at the Fermi energy,  $v_f$  is the Fermi velocity and  $v_f \tau_\kappa$  is the transport mean-free-path for heat conduction, with  $\tau_\kappa \sim \tau_{\text{in}} \sim T^{-2}$ . Thus, heat transport becomes very efficient in pure  $^3\text{He}$  with  $\kappa \sim 1/T$ .<sup>1,16</sup>

In aerogel, elastic collisions of  $^3\text{He}$  quasiparticles with the silica strands lead to a temperature-independent contribution to the mean free path and hence the quasiparticle scattering rate. Thus, at sufficiently low temperatures, transport currents are limited by elastic scattering from the aerogel, whereas inelastic scattering of quasiparticles dominates at high temperatures. There is an intermediate regime where both mechanisms are important. The cross-over temperature separating these regimes is estimated from the inelastic collision rate in the pure  $^3\text{He}$  in Eq. (1) and the  $mfp$  of the aerogel,  $\ell$ , which provides an estimate for the elastic collision rate,

$$\frac{1}{\tau_{\text{el}}} = \frac{v_f}{\ell} = \text{constant}. \quad (3)$$

Estimating  $\tau_\kappa$  from Eqs. (1) and (3) gives,

$$\kappa = \frac{1}{3} \bar{c}_v v_f^2 \tau_\kappa \sim \begin{cases} T & , \quad T < T_\star \\ 1/T & , \quad T > T_\star. \end{cases} \quad (4)$$

The cross-over temperature,  $T_\star$ , defined by  $\tau_{\text{in}}(T_\star) = \tau_{\text{el}}$ , is given by<sup>29</sup>

$$T_\star = \frac{8E_f/k_B}{\sqrt{\pi k_f \ell \langle W \rangle}}, \quad (5)$$

where  $\langle \bar{W} \rangle$  is the dimensionless quasiparticle transition probability averaged over the Fermi surface (Eq. 171 of the appendix). For 98% porosity aerogel we estimate  $\ell \approx 1700 \text{ \AA}$ ,<sup>38</sup> and thus  $T_\star \approx 18 \text{ mK}$  at  $p = 15 \text{ bar}$  (see Fig. 1).

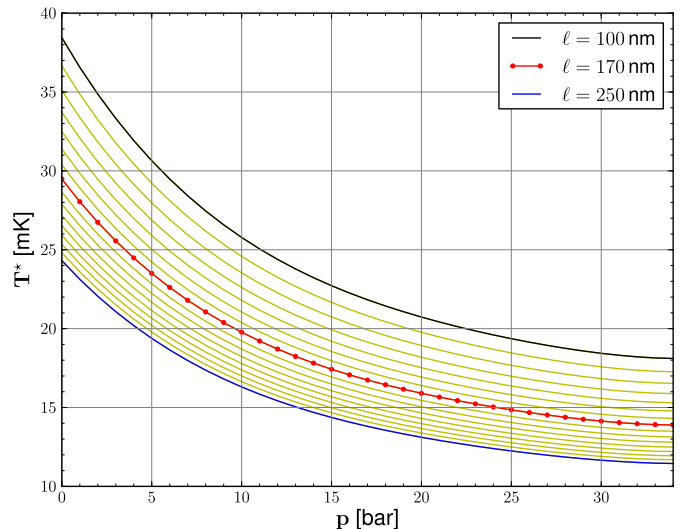


FIG. 1: Cross-over temperature vs. pressure for aerogels characterized by the  $mfp$  as defined by Eqs. 1-5. The curves correspond to  $\ell = 100 - 250 \text{ nm}$  spaced by  $10 \text{ nm}$ . The red curve is for  $\ell = 170 \text{ nm}$  ( $\rho \approx 98\%$ ). The cross-over temperature is obtained from Eq. 5 with  $\langle W \rangle$  given by Eqs. (174-177), Table I (see the appendix in Sec. V), and the relevant Fermi-liquid parameters from Refs. 17,19.

The cross-over from the high-temperature regime dominated by inelastic scattering to the low-temperature regime dominated by elastic scattering off the aerogel is characteristic of all transport processes for  $^3\text{He}$  in aerogel.<sup>25,29,31,39</sup> Below we report theoretical results for the heat transport coefficient of liquid  $^3\text{He}$ -aerogel, in the normal state, over the broad temperature range,  $T_c \leq T \ll E_f/k_B$ . Since the bulk properties of  $^3\text{He}$  are well known, measurements of the transport coefficients can provide quantitative information on the effects of disorder on the transport of  $^3\text{He}$  quasiparticles through aerogel.

## II. TRANSPORT THEORY

In normal liquid  $^3\text{He}$  at low temperatures the transport of mass, energy and magnetization is carried predominantly by fermionic quasiparticles, whose distribution in phase space,  $n_{\mathbf{p}\sigma}$ , is governed by the Boltzmann-Landau transport equation,<sup>5,9</sup>

$$\frac{\partial n_p}{\partial t} + \nabla_{\mathbf{p}} \varepsilon_p \cdot \nabla_{\mathbf{r}} n_p - \nabla_{\mathbf{p}} n_p \cdot \nabla_{\mathbf{r}} \varepsilon_p = \left( \frac{\partial n_p}{\partial t} \right)_{\text{coll}} \equiv I_p, \quad (6)$$

where  $p = (\mathbf{p}, \sigma)$  denotes the momentum and spin of the quasiparticles. For spin-independent transport the quasiparticle energy

$$\varepsilon_{\mathbf{p}} = \epsilon_{\mathbf{p}} + \delta \varepsilon_{\mathbf{p}}(\mathbf{r}, t) + u_{\text{ext}}(\mathbf{p}, \mathbf{r}, t), \quad (7)$$

is the sum of the equilibrium excitation energy,  $\epsilon_{\mathbf{p}}$ , the coupling to an external scalar or vector potential,  $u_{\text{ext}}(\mathbf{p}, \mathbf{r}, t)$ , and the Landau molecular field energy. The latter arises from the interaction of a quasiparticle with the distribution of non-equilibrium quasiparticles,

$$\delta\epsilon_{\mathbf{p}} = \sum_{\mathbf{p}'\sigma'} f_{\mathbf{p},\mathbf{p}'} \delta n_{\mathbf{p}'}, \quad (8)$$

where  $\delta n_{\mathbf{p}}$  is the deviation of the distribution function from (global) equilibrium,

$$\delta n_{\mathbf{p}} = n_{\mathbf{p}} - n_0(\epsilon_{\mathbf{p}}). \quad (9)$$

For small disturbances from equilibrium the derivative of the equilibrium distribution function,

$$-\frac{\partial n_0}{\partial \epsilon_{\mathbf{p}}} = \frac{1}{4k_B T} \text{sech}^2\left(\frac{\epsilon_{\mathbf{p}} - \mu}{2k_B T}\right), \quad (10)$$

confines the excitations to states that lie near the Fermi surface,  $\epsilon_{\mathbf{p}_f} = \mu$ . The interaction energy between two quasiparticles is given by  $f_{\mathbf{p},\mathbf{p}'}$ , and in contrast to the distribution function, varies slowly with  $|\mathbf{p}|$  in the vicinity of the Fermi surface. We can typically evaluate  $f_{\mathbf{p},\mathbf{p}'}$ , as well as the density of states,  $N(\epsilon)$ , on the Fermi surface, i.e.  $N(\epsilon) \simeq N_f$ , and  $2N_f f(p_f \hat{\mathbf{p}}, p_f \hat{\mathbf{p}}') = F(\hat{\mathbf{p}} \cdot \hat{\mathbf{p}}') = \sum_{\ell} F_{\ell} P_{\ell}(\hat{\mathbf{p}} \cdot \hat{\mathbf{p}}')$ . The latter equality defines the dimensionless Landau parameters.

### A. Collision Integrals

The right side of the transport equation,  $I_p$ , represents the change in the distribution function resulting from collision processes. We consider two scattering processes for  $^3\text{He}$  in aerogel: (i) elastic collisions of quasiparticles with “impurities” representing the aerogel strands, and (ii) inelastic collisions between quasiparticles. The development of the transport theory for  $^3\text{He}$ -aerogel presented below, particularly the reduction of the transport equation in the low temperature limit, parallels that development by Baym and Pethick in their review on transport in pure liquid  $^3\text{He}$ ,<sup>8</sup> and extends Brooker and Sykes’ work on the transport coefficients of Fermi liquids.<sup>37</sup>

In our case the effects of aerogel scattering enter through a contribution to the collision integral. For quasiparticle scattering by the aerogel strands

$$I_{p_1}^{\text{el}} = -\frac{2}{V} \sum_{p_2} w(p_1, p_2) \delta(\epsilon_1 - \epsilon_2) [n_{p_1} - n_{p_2}], \quad (11)$$

where  $w(p_1, p_2)$  is the transition rate for scattering of quasiparticles by the aerogel.

For inelastic quasiparticle-quasiparticle collisions at low temperatures,  $k_B T \ll E_f$ , only binary collisions are important. We denote  $\mathfrak{t}(p_1, p_2; p_3, p_4)$  as the scattering amplitude for

binary collisions between quasiparticles with momenta and spin  $p_i = (\mathbf{p}_i, \sigma_i)$ . The labels  $p_1$  and  $p_2$  refer to initial states while  $p_3$  and  $p_4$  refer to final states. Fermi’s Golden Rule for the transition rate  $(p_1, p_2) \rightarrow (p_3, p_4)$  is:

$$\Gamma = \frac{2\pi}{\hbar} |\mathfrak{t}(p_1, p_2; p_3, p_4)|^2 \delta(\epsilon_1 + \epsilon_2 - \epsilon_3 - \epsilon_4). \quad (12)$$

For a translationally invariant system with spin-rotation invariant interactions between quasiparticles the transition rate includes momentum- and spin-conserving delta functions,

$$\Gamma = \frac{1}{V^2} W(p_1, p_2; p_3, p_4) \delta_{\mathbf{p}_1 + \mathbf{p}_2, \mathbf{p}_3 + \mathbf{p}_4} \delta_{\sigma_1 + \sigma_2, \sigma_3 + \sigma_4} \delta(\epsilon_1 + \epsilon_2 - \epsilon_3 - \epsilon_4). \quad (13)$$

where  $W$  is a smooth function of  $\mathbf{p}_i$ .

The collision integral for binary scattering includes the phase space factors for collisions that both increase and decrease the population of the state  $p_1$  (scattering “in” and scattering “out”). In particular,

$$I_{p_1}^{\text{in}} = - \sum_{p_2, p_3, p_4} \Gamma(p_1, p_2; p_3, p_4) \times [n_{p_1} n_{p_2} (1 - n_{p_3})(1 - n_{p_4}) - (1 - n_{p_1})(1 - n_{p_2}) n_{p_3} n_{p_4}]. \quad (14)$$

The sum over final states  $(p_3, p_4)$  is restricted to avoid double counting of equivalent states of identical particles related by exchange of  $p_3 \leftrightarrow p_4$ .

The collision integral vanishes when evaluated with a local equilibrium distribution function, i.e.  $I[n_p^{\text{le}}] \equiv 0$ . For the elastic scattering contribution to the collision integral (Eq. 11) this identity is obvious. For the inelastic collision integral it is less so, but follows from the identity,

$$\delta(\epsilon_{p_1} + \epsilon_{p_2} - \epsilon_{p_3} - \epsilon_{p_4}) \times [n_0(\epsilon_{p_1}) n_0(\epsilon_{p_2})(1 - n_0(\epsilon_{p_3}))(1 - n_0(\epsilon_{p_4})) - n_0(\epsilon_{p_3}) n_0(\epsilon_{p_4})(1 - n_0(\epsilon_{p_1}))(1 - n_0(\epsilon_{p_2}))] = 0, \quad (15)$$

where  $n_0(\epsilon) = 1/(e^{\beta(\epsilon - \mu)} + 1)$  is the Fermi distribution. This identity is a consequence of local equilibrium and the condition of detailed balance between the scattering “in” and scattering “out” contributions to the collision rate.

Although translational invariance is violated by the presence of the aerogel medium, the aerogel is sufficiently dilute that the scattering rate by the aerogel impurities is typically small compared to excitation energies in the normal state, i.e.  $\hbar/\tau_{\text{el}} \ll k_B T$ .<sup>41</sup> In this limit the effects of aerogel scattering on the intermediate states that enter the inelastic collision integral can be neglected. Thus, momentum conservation holds for the binary collision integral for normal  $^3\text{He}$  in high porosity aerogels. At lower temperatures, e.g. in the superfluid phase, or for lower porosity aerogels, this approximation breaks down. This limit requires a microscopic treatment of the effects of aerogel scattering on inelastic collision processes which is outside the scope of the phenomenological Boltzmann-Landau transport theory.

### B. Linearized Transport Equation

The transport coefficients of liquid  $^3\text{He}$  in aerogel are calculated from solutions of the *linearized* transport equation in steady-state. The particular solution depends on the nonequilibrium conditions that are established. For small deviations from equilibrium the nonequilibrium steady state is specified by a *local equilibrium* distribution function,

$$n_p^{l.e.} = \frac{1}{1 + e^{(\varepsilon_p(\mathbf{r}) - \mu(\mathbf{r}))/k_B T(\mathbf{r})}}, \quad (16)$$

parametrized by a local temperature,  $T(\mathbf{r})$ , chemical potential,  $\mu(\mathbf{r})$  and quasiparticle energy,  $\varepsilon_p(\mathbf{r})$ . The transport equation naturally separates by expanding about this local equilibrium distribution,

$$\delta \bar{n}_p = n_p - n_p^{l.e.}, \quad (17)$$

because the collision integral vanishes under the conditions of local equilibrium,  $I_p[n_p^{l.e.}] \equiv 0$ . The linearized transport equation becomes,

$$\mathbf{v}_p \cdot \nabla_{\mathbf{r}} n_p^{l.e.} - \left( \frac{\partial n_p^{l.e.}}{\partial \varepsilon_p} \right) \mathbf{v}_p \cdot \nabla_{\mathbf{r}} \varepsilon_p = \delta I_p[\delta \bar{n}_p]. \quad (18)$$

The left side of Eq. (18) supplies the driving terms, e.g.  $\nabla \mu$  and  $\nabla T$ , for the collision terms on the right side that act to restore equilibrium. Using Eq. (16) the linearized transport equation reduces to

$$- \left( \frac{\partial n_0}{\partial \varepsilon_p} \right) \mathbf{v}_p \cdot \left[ \left( \frac{\varepsilon_p - \mu}{T} \right) \nabla T + \nabla \mu \right] = \delta I_p[\delta \bar{n}_p], \quad (19)$$

where  $\delta I_p$  is the collision integral to linear order in  $\delta \bar{n}_p$ .

### C. Quasiparticle Currents

The mass and heat currents are determined by the solution for  $\delta \bar{n}_p$  of Eq. (19). In particular, the mass current is given by

$$\mathbf{j}_m = \sum_{\mathbf{p}\sigma} m^* \mathbf{v}_p \delta \bar{n}_{\mathbf{p}\sigma}, \quad (20)$$

where  $m^* = p_f/v_f$  is the quasiparticle effective mass. This form for the mass current is applicable to interacting Fermi liquids which are Galilean invariant.<sup>9</sup> In pure liquid  $^3\text{He}$  quasiparticle-quasiparticle interactions which give rise to the enhancement of the Fermionic mass are Galilean invariant. For liquid  $^3\text{He}$ -aerogel Galilean invariance is violated by quasiparticle scattering off the aerogel. However, the non-Galilean contribution to the effective mass is of the order of concentration of scattering centers,  $n_s/n \ll 1$ , and thus negligible compared to the quasiparticle-quasiparticle effective mass enhancement.

Similarly, the quasiparticle heat current is given by the transport of excitations with energy,  $\xi_p = \varepsilon_p - \mu$ ,

$$\mathbf{j}_q = \sum_{\mathbf{p}\sigma} \xi_p \mathbf{v}_p \delta \bar{n}_{\mathbf{p}\sigma}. \quad (21)$$

### D. Elastic Scattering Limit

Transport properties of normal  $^3\text{He}$  in aerogel at sufficiently low temperatures, i.e.  $T \ll T_*$ , are limited by elastic scattering of quasiparticles by the aerogel structure. In this limit the transport equation is given by Eq. (19) with the collision term of Eq. (11). The integral equation for  $\delta \bar{n}_p$  is

$$- \left( \frac{\partial n_0}{\partial \xi_p} \right) \mathbf{v}_p \cdot \mathbf{Z}(\xi_p) = - \sum_{\mathbf{p}'\sigma'} w(\mathbf{p}, \mathbf{p}') \delta(\xi_p - \xi_{p'}) \times [\delta \bar{n}_{\mathbf{p}\sigma} - \delta \bar{n}_{\mathbf{p}'\sigma'}], \quad (22)$$

where

$$\mathbf{Z}(\xi_p) = \left[ \left( \frac{\xi_p}{T} \right) \nabla T + \nabla \mu \right]. \quad (23)$$

The solutions to Eq. (22) are determined by the energy and momentum dependences of the driving term and are familiar from the theory of electron-impurity scattering in metals.<sup>3</sup> To proceed further we need the  $^3\text{He}$  quasiparticle-aerogel scattering probability,  $w(p, p')$ .

### E. Elastic Scattering Model

We model the aerogel as a distribution of local scattering centers represented by the potential,  $U(\mathbf{r}) = \sum_i u(\mathbf{r} - \mathbf{R}_i)$ . The terms  $u(\mathbf{r} - \mathbf{R}_i)$  represent the potential provided by the aerogel scattering centers at the *fixed* positions,  $\{\mathbf{R}_i | i = 1 \dots N_s\}$ . For a random distribution of uncorrelated scattering centers the rate is proportional to the mean number density of scattering centers,  $n_s = N_s/V$ . In the Born approximation the transition rate is related to the matrix elements of  $u$ ,

$$w(\mathbf{p}\sigma; \mathbf{p}'\sigma') = n_s \frac{2\pi}{\hbar} |\langle \mathbf{p}'\sigma' | u | \mathbf{p}\sigma \rangle|^2. \quad (24)$$

For stronger scattering the potential  $u$  is replaced by the  $t$ -matrix for quasiparticle scattering by aerogel strands.<sup>34</sup>

We shall assume that the scattering by the aerogel is *non-magnetic*. This should be sufficient for describing transport processes in zero field, particularly if the aerogel strands are “coated” with a layer of solid  $^4\text{He}$ . However, it is known that  $^3\text{He}$  atoms form a highly polarizable solid layer on the surface of the aerogel strands and that these nuclear spins exhibit a Curie-like spin susceptibility.<sup>36</sup> Thus, spin-exchange scattering of  $^3\text{He}$  quasiparticles by localized and polarizable

$^3\text{He}$  spins may be relevant to magnetic transport processes and transport in relatively low magnetic fields. The simplest scattering model for  $^3\text{He}$ -aerogel assumes the  $^3\text{He}$  quasiparticles interact with the aerogel via an isotropic scattering potential.<sup>38</sup> There is no preferred direction within the aerogel and the scattering probability depends on the relative orientation of the initial and final quasiparticle momenta. In this case,

$$w(\mathbf{p}, \mathbf{p}') = w(\hat{\mathbf{p}} \cdot \hat{\mathbf{p}}'; \xi_{\mathbf{p}}) = \sum_{l \geq 0} w_l(\xi_{\mathbf{p}}) \mathcal{P}_l(\hat{\mathbf{p}} \cdot \hat{\mathbf{p}}'), \quad (25)$$

where  $w_l(\xi_{\mathbf{p}})$  is the scattering probability for quasiparticles with relative orbital angular momentum  $l$ , and  $\mathcal{P}_l(x)$  is the corresponding Legendre polynomial. Note that  $|\mathbf{p}| = |\mathbf{p}'|$  for elastic scattering, and we have parametrized the functional dependence of  $w(\mathbf{p}, \mathbf{p}')$  on  $|\mathbf{p}|$  by the energy  $\xi_{\mathbf{p}} = v_f(|\mathbf{p}| - p_f)$  measured relative to the Fermi surface. The probabilities for scattering in the orbital channels are proportional to,

$$w_l(\xi_{\mathbf{p}}) \equiv \frac{1}{(2l+1)} \int_{-1}^{+1} \frac{dx}{2} w(x; \xi_{\mathbf{p}}) \mathcal{P}_l(x), \quad (26)$$

which vary smoothly with  $\xi_{\mathbf{p}}$  on the scale of  $E_f$ .

For an isotropic scattering medium we make the *ansatz*,

$$\delta \bar{n}_{\mathbf{p}} = \left( \frac{\partial n_0}{\partial \xi_{\mathbf{p}}} \right) [\mathbf{v}_{\mathbf{p}} \tau_{\text{el}}(\xi_{\mathbf{p}})] \cdot \mathbf{Z}(\xi_{\mathbf{p}}). \quad (27)$$

The momentum sum is represented as

$$\sum_{\mathbf{p}'} (\dots) = \int \frac{d\Omega_{\hat{\mathbf{p}}'}}{4\pi} \int d\xi_{\mathbf{p}'} N(\xi_{\mathbf{p}'}) (\dots). \quad (28)$$

The terms  $(\partial n_0 / \partial \xi_{\mathbf{p}})$  and  $\delta(\xi_{\mathbf{p}} - \xi_{\mathbf{p}'})$  confine  $|\mathbf{p}'| = |\mathbf{p}| \simeq p_f + \xi_{\mathbf{p}}/v_f$ , so we obtain

$$\frac{1}{\tau_{\text{el}}(\xi_{\mathbf{p}})} = 2N(\xi_{\mathbf{p}}) \langle w(\hat{\mathbf{p}} \cdot \hat{\mathbf{p}}'; \xi_{\mathbf{p}}) (1 - \hat{\mathbf{p}} \cdot \hat{\mathbf{p}}') \rangle_{\hat{\mathbf{p}}'}, \quad (29)$$

where  $\langle \dots \rangle_{\hat{\mathbf{p}}'} \equiv \int \frac{d\Omega_{\hat{\mathbf{p}}'}}{4\pi} (\dots)$ . We introduce the scattering rate for orbital channel  $l$ ,

$$\frac{1}{\tau_l(\xi_{\mathbf{p}})} \equiv \frac{2N(\xi_{\mathbf{p}})}{(2l+1)} \int_{-1}^{+1} \frac{dx}{2} w(x; \xi_{\mathbf{p}}) \mathcal{P}_l(x) = 2N(\xi_{\mathbf{p}}) w_l(\xi_{\mathbf{p}}), \quad (30)$$

and express the transport scattering rate in terms of the  $l = 0$  and  $l = 1$  (s- and p-wave) scattering rates,

$$\frac{1}{\tau_{\text{el}}(\xi_{\mathbf{p}})} = \frac{1}{\tau_0(\xi_{\mathbf{p}})} - \frac{1}{\tau_1(\xi_{\mathbf{p}})}. \quad (31)$$

Note that the density of states,  $N(\xi_{\mathbf{p}})$ , and the scattering probabilities,  $w_l(\xi_{\mathbf{p}})$ , vary slowly with excitation energy on the scale of the Fermi energy. Thus, for many cases of interest we can safely neglect the energy dependence of the scattering rate and evaluate  $\tau_{\text{el}}(\xi_{\mathbf{p}}) \simeq \tau_{\text{el}}(0) \equiv \tau_{\text{el}}$ .

In particular, the mass current induced by a pressure gradient at constant temperature is determined by the quasiparticle *mobility* defined by  $\mathbf{j}_m = -\nu \nabla \mu$ . For  $k_B T \ll E_f$  Eq. (10) is sharply peaked at the Fermi energy, and the quasiparticle mobility calculated from Eqs. (20) and (27) is to leading order in  $T/E_f$ ,

$$\nu = \frac{2}{3} N_f p_f (v_f \tau_{\text{el}}), \quad (32)$$

which has the intuitive interpretation of transport of momentum  $p_f$  over a distance of order the *mfp*,  $\ell = v_f \tau_{\text{el}}$ , within the aerogel. Similarly, the heat current, Eq. (21), induced by an temperature gradient,  $\mathbf{j}_q = -\kappa \nabla T$ , defines the thermal conductivity, which to leading order in  $T/E_f$  is given by,

$$\kappa_{\text{el}} = \frac{2\pi^2}{9} k_B N_f (v_f k_B T) \ell, \quad (33)$$

and also has the simple interpretation as the flux of thermal energy  $v_f k_B T$  transported over a distance of order  $\ell$ .

## F. Two Channel Collision Integral

For higher temperatures, i.e.  $T \gtrsim T_*$ , both elastic and inelastic collision processes limit transport currents. The transport coefficients are then calculated from

$$- \left( \frac{\partial n_0}{\partial \xi_{p_1}} \right) \mathbf{v}_{p_1} \cdot \left[ \left( \frac{\xi_{p_1}}{T} \right) \nabla T + \nabla \mu \right] = \delta I_{p_1}^{\text{in}} + \delta I_{p_1}^{\text{el}}, \quad (34)$$

where the right side of Eq. (34) contains the linearized collision integrals for both inelastic and elastic scattering. The elastic collision integral follows immediately from Eq. (11),

$$\delta I_{p_1}^{\text{el}} = - \sum_{p_2} w(p_1, p_2) [\delta \bar{n}_{p_1} - \delta \bar{n}_{p_2}] \delta(\xi_{p_1} - \xi_{p_2}). \quad (35)$$

Since the driving terms in Eq. (34) are confined to excitation energies within  $k_B T$  of the Fermi energy we express

$$\delta \bar{n}_{p_i} = \left( \frac{\partial n_0}{\partial \xi_{p_i}} \right) \psi_{p_i}, \quad (36)$$

where  $\psi_{p_i}$  measures the deviation of the equilibrium distribution for quasiparticles with excitation energy  $\xi_{p_i}$  at the point  $\hat{\mathbf{p}}_i$  on the Fermi surface.

For  $|\xi_{\mathbf{p}_1}| \ll E_f$  energy conservation, combined with the phase-space restriction required by the Fermi distribution factors in Eq. (35), forces the scattered excitation energy to be confined to the low-energy shell, i.e.  $|\xi_{\mathbf{p}_2}| \lesssim k_B T$ . Thus, slowly varying functions of  $\mathbf{p}_i$  can be evaluated with momenta,  $|\mathbf{p}_1| = |\mathbf{p}_2| \simeq p_f + \xi_{\mathbf{p}_1}/v_f$ , i.e. in close vicinity of the Fermi momentum. The scattering rate  $w$  reduces to a function of the *directions* of the momenta for incident and scattered excitations with excitation energies near the Fermi



energy,  $w(\mathbf{p}_1, \mathbf{p}_2) \rightsquigarrow w(\hat{\mathbf{p}}_1, \hat{\mathbf{p}}_2; \xi_{\mathbf{p}_1})$ . For the isotropic scattering model and a driving term proportional to  $\mathbf{v}_{\mathbf{p}_i} \cdot \nabla T$  we set

$$\psi_{\mathbf{p}_i} = \mathbf{v}_{\mathbf{p}_i} \cdot \nabla T \varphi(\xi_{\mathbf{p}_i}), \quad (37)$$

in which case the elastic collision integral becomes,

$$\delta I_{p_1}^{\text{el}} = \frac{\mathbf{v}_{\mathbf{p}_1} \cdot \nabla T}{T} n_0(\xi_{\mathbf{p}_1})(1 - n_0(\xi_{\mathbf{p}_1})) \frac{1}{\tau_{\text{el}}(\xi_{\mathbf{p}_1})} \varphi(\xi_{\mathbf{p}_1}). \quad (38)$$

Linearizing the inelastic collision rate in Eq. (14), and making use of Eq. (15) yields,

$$\begin{aligned} \delta I_{p_1}^{\text{in}} = & \frac{1}{T} \sum_{p_2, p_3, p_4} W(p_1, p_2; p_3, p_4) \delta_{\sum_i \mathbf{p}_i} \delta_{\sum_i \sigma_i} \delta_{\sum_i \xi_{p_i}} \\ & \times [n_0(\xi_{p_1}) n_0(\xi_{p_2})(1 - n_0(\xi_{p_3}))(1 - n_0(\xi_{p_4}))] \\ & [\psi_{p_1} + \psi_{p_2} - \psi_{p_3} - \psi_{p_4}]. \end{aligned} \quad (39)$$

Here we consider an un-polarized Fermi liquid in which the only spin-dependent interactions are those that arise from exchange symmetry. In this case,  $\xi_{p_i} = \xi_{\mathbf{p}_i}$  and the distribution functions are independent of  $\sigma_i$ . Thus, we can carry out the sum over the spin states  $\sigma_{2,3,4}$ . We can also eliminate one of the momentum sums, resulting in,

$$\begin{aligned} \delta I_{p_1}^{\text{in}} = & \frac{2}{T} \sum_{\mathbf{p}_2, \mathbf{p}_3} W(\mathbf{p}_1, \mathbf{p}_2; \mathbf{p}_3, \mathbf{p}_4) \delta(\xi_{\mathbf{p}_1} + \xi_{\mathbf{p}_2} - \xi_{\mathbf{p}_3} - \xi_{\mathbf{p}_4}) \\ & \times [n_0(\xi_{\mathbf{p}_1}) n_0(\xi_{\mathbf{p}_2})(1 - n_0(\xi_{\mathbf{p}_3}))(1 - n_0(\xi_{\mathbf{p}_4}))] \\ & \times [\psi_{\mathbf{p}_1} + \psi_{\mathbf{p}_2} - \psi_{\mathbf{p}_3} - \psi_{\mathbf{p}_4}], \end{aligned} \quad (40)$$

where  $\mathbf{p}_4 = \mathbf{p}_1 + \mathbf{p}_2 - \mathbf{p}_3$  and

$$W = \frac{1}{4} W_{\uparrow\uparrow} + \frac{1}{2} W_{\uparrow\downarrow}, \quad (41)$$

is the spin-averaged scattering rate;  $W_{\uparrow\uparrow}$  is the scattering rate for  $\sigma_1 = \sigma_2 = \uparrow$  and  $W_{\uparrow\downarrow}$  is the rate for  $\sigma_1 = -\sigma_2 = \uparrow$ . The weight factors take into account the restriction to avoid double counting of equivalent states, so the remaining momentum sums over  $\mathbf{p}_3$  and  $\mathbf{p}_4$  are unrestricted.<sup>9</sup>

For  $|\xi_{\mathbf{p}_1}| \ll E_f$  the energy and momentum conservation laws, combined with the phase-space restrictions required by the Fermi distribution factors in Eq. (40), force all excitation energies to be confined to the low-energy shell, i.e.  $|\xi_{\mathbf{p}_i}| \lesssim k_B T$ . In this limit slowly varying functions of  $\mathbf{p}_i$  can be evaluated on the Fermi surface. Thus, the scattering rate  $W$  becomes a function of the *directions* of the momenta for quasiparticles on the Fermi surface,

$$W(\mathbf{p}_1, \mathbf{p}_2; \mathbf{p}_3, \mathbf{p}_4) \rightsquigarrow W(\hat{\mathbf{p}}_1, \hat{\mathbf{p}}_2; \hat{\mathbf{p}}_3, \hat{\mathbf{p}}_4), \quad (42)$$

and the momentum sums can be approximated by

$$\sum_{\mathbf{p}_i} (\dots) \rightsquigarrow N_f \int \frac{d\Omega_{\hat{\mathbf{p}}_i}}{4\pi} \int d\xi_{\mathbf{p}_i} (\dots). \quad (43)$$

To carry out the angular integrations we adopt Abrikosov and Khalatnikov's parametrization<sup>5</sup> of  $W$  in terms of the angle  $\theta$  between the two incoming momenta, and  $\phi$ , the scattering angle between the planes defined by  $\mathbf{n} = \hat{\mathbf{p}}_1 \times \hat{\mathbf{p}}_2$  and  $\mathbf{n}' = \hat{\mathbf{p}}_3 \times \hat{\mathbf{p}}_4$ . The integration over the direction  $\hat{\mathbf{p}}_3$  is expressed in terms of angles relative to the conserved direction of the total momentum,  $\mathbf{P} = \mathbf{p}_1 + \mathbf{p}_2$ ,

$$\int \frac{d\Omega_{\hat{\mathbf{p}}_3}}{4\pi} (\dots) = \int_0^{2\pi} \frac{d\phi_3}{2\pi} \int_{-1}^{+1} \frac{d(\cos \alpha)}{2} (\dots). \quad (44)$$

Since  $p_4 = \sqrt{P^2 + p_3^2 - 2\mathbf{P} \cdot \mathbf{p}_3}$  we have  $dp_4 = (p_3/p_4) P d(\cos \alpha)$ , and for momenta near the Fermi surface,  $P \simeq 2p_f \cos(\theta/2)$ . Thus,

$$d(\cos \alpha) \simeq \frac{d\xi_{\mathbf{p}_4}}{2v_f p_f \cos(\theta/2)}. \quad (45)$$

Also, the azimuthal angle  $\phi_3$  is the scattering angle up to a fixed but arbitrary constant, thus,  $d\phi_3 = d\phi$ . In the case of the integration over the incoming momentum direction  $\hat{\mathbf{p}}_2$  we choose the remaining momentum direction  $\mathbf{p}_1$  as the polar axis,

$$\int \frac{d\Omega_{\hat{\mathbf{p}}_2}}{4\pi} (\dots) = \int_0^{2\pi} \frac{d\phi_2}{2\pi} \int_{-1}^{+1} \frac{d(\cos \theta)}{2} (\dots). \quad (46)$$

The binary collision integral then reduces to

---


$$\begin{aligned} \delta I_{p_1}^{\text{in}} = & \frac{2}{T} N_f^2 \left( \frac{1}{2v_f p_f} \right) \int d\xi_{\mathbf{p}_2} \int d\xi_{\mathbf{p}_3} \int d\xi_{\mathbf{p}_4} \delta(\xi_{\mathbf{p}_1} + \xi_{\mathbf{p}_2} - \xi_{\mathbf{p}_3} - \xi_{\mathbf{p}_4}) [n_0(\xi_{\mathbf{p}_1}) n_0(\xi_{\mathbf{p}_2})(1 - n_0(\xi_{\mathbf{p}_3}))(1 - n_0(\xi_{\mathbf{p}_4}))] \\ & \times \int_{-1}^{+1} \frac{d(\cos \theta)}{2} \int_0^{2\pi} \frac{d\phi}{2\pi} \left( \frac{W(\theta, \phi)}{2 \cos(\theta/2)} \right) \int_0^{2\pi} \frac{d\phi_2}{2\pi} [\psi_{\mathbf{p}_1} + \psi_{\mathbf{p}_2} - \psi_{\mathbf{p}_3} - \psi_{\mathbf{p}_4}]. \end{aligned} \quad (47)$$


---

The inhomogeneous terms of the linearized transport equation dictate the symmetry of the solution with respect to

excitation energy,  $\xi_{\mathbf{p}_1} \rightarrow -\xi_{\mathbf{p}_1}$ , and momentum direction,  $\hat{\mathbf{p}}_1$ . We separate the angular and energy dependences of

the non-equilibrium distribution function with the *ansatz*,  $\psi_{\mathbf{p}_i} = \psi_{\mathbf{p}_i}^{(+)} + \psi_{\mathbf{p}_i}^{(-)}$ ,

$$\psi_{\mathbf{p}_i}^{(+)} = \mathbf{v}_{\mathbf{p}_i} \cdot \nabla \mu \varphi^{(+)}(\xi_{\mathbf{p}_i}) \quad (48)$$

$$\psi_{\mathbf{p}_i}^{(-)} = \mathbf{v}_{\mathbf{p}_i} \cdot \nabla T \varphi^{(-)}(\xi_{\mathbf{p}_i}), \quad (49)$$

where  $\varphi^{(\pm)}(\xi_{\mathbf{p}_i}) = \pm \varphi^{(\pm)}(-\xi_{\mathbf{p}_i})$ . We can now carry out the integration over  $\phi_2$  for each term in Eq. (47),

$$\int_0^{2\pi} \frac{d\phi_2}{2\pi} \psi_{\mathbf{p}_i} = x_i \mathbf{v}_{\mathbf{p}_1} \cdot \left[ \nabla \mu \varphi^{(+)}(\xi_{\mathbf{p}_i}) + \nabla T \varphi^{(-)}(\xi_{\mathbf{p}_i}) \right], \quad (50)$$

where the direction cosines,  $x_i = \hat{\mathbf{p}}_i \cdot \mathbf{p}_1$  for  $i = 2, 3, 4$ , are simply related to  $(\theta, \phi)$ . The angular integrations decouple from the energy integrations which are confined to the low-energy shell near the Fermi surface. We define the average scattering rate

$$\langle W \rangle \equiv \int_{-1}^{+1} \frac{d(\cos \theta)}{2} \int_0^{2\pi} \frac{d\phi}{2\pi} \left( \frac{W(\theta, \phi)}{2 \cos(\theta/2)} \right), \quad (51)$$

as well as the weighted averages,  $r_i = \langle x_i W \rangle / \langle W \rangle$ . Changing  $\xi_{\mathbf{p}_3, \mathbf{p}_4} \rightarrow -\xi_{\mathbf{p}_3, \mathbf{p}_4}$  the resulting collision integral reduces to

$$\delta I_{p_1}^{\text{in}(\pm)} = \frac{1}{T} \frac{N_f^2}{p_f v_f} \langle W \rangle \mathbf{v}_{\mathbf{p}_1} \cdot \left( \frac{\nabla \mu}{\nabla T} \right) \times n_0(\xi_{\mathbf{p}_1}) \times \left[ I(\xi_{\mathbf{p}_1}) \varphi^{(\pm)}(\xi_{\mathbf{p}_1}) + \lambda^{(\pm)} \int d\xi_{\mathbf{p}_2} n_0(\xi_{\mathbf{p}_2}) K(\xi_{\mathbf{p}_1} + \xi_{\mathbf{p}_2}) \varphi^{(\pm)}(\xi_{\mathbf{p}_2}) \right], \quad (52)$$

where

$$\begin{aligned} K(\xi) &= \int d\xi_3 \int d\xi_4 \delta(\xi + \xi_3 + \xi_4) n_0(\xi_3) n_0(\xi_4) \\ &= \left( \frac{\xi}{1 - e^{-\xi/T}} \right), \end{aligned} \quad (53)$$

$$\begin{aligned} I(\xi) &= \int d\xi_2 n_0(\xi_2) K(\xi + \xi_2) \\ &= \frac{1}{2} (\pi^2 T^2 + \xi^2) (1 - n_0(\xi)), \end{aligned} \quad (54)$$

and  $\lambda^{(\pm)}$  are given by,

$$\lambda^{(\pm)} \equiv r_2 \mp (r_3 + r_4) = \left\{ \frac{-1}{\langle W(1 + 2 \cos \theta) \rangle / \langle W \rangle} \right\}. \quad (55)$$

It is then convenient to measure the excitation energy in units of  $T$ , i.e. set  $t_i \equiv \xi_{\mathbf{p}_i}/T$ , for  $i = 1, 2, 3, 4$ . The resulting inelastic collision integrals reduce to

$$\delta I_{p_1}^{\text{in}(\pm)} = \frac{1}{T} n_0(t_1) \mathbf{v}_{\mathbf{p}_1} \cdot \left( \frac{\nabla \mu}{\nabla T} \right) \frac{1}{\tau_{\text{in}}} \times \left[ \frac{1}{2} (1 - n_0(t_1)) (\pi^2 + t_1^2) \varphi^{(\pm)}(t_1) + \lambda^{(\pm)} \int dt_2 n_0(t_2) \frac{t_1 + t_2}{\sinh\left(\frac{t_1 + t_2}{2}\right)} \varphi^{(\pm)}(t_2) \right], \quad (56)$$

where  $1/\tau_{\text{in}}$  is the quasiparticle-quasiparticle collision rate given in Eq. (1). These same transformations applied to the elastic collision integral in Eq. (38) yield,

$$\delta I_{p_1}^{\text{el}(\pm)} = \frac{1}{T} n_0(t_1) (1 - n_0(t_1)) \mathbf{v}_{\mathbf{p}_1} \cdot \left( \frac{\nabla \mu}{\nabla T} \right) \frac{1}{\tau_{\text{el}}} \times \varphi^{(\pm)}(t_1), \quad (57)$$

where  $1/\tau_{\text{el}}$  is the rate for quasiparticles on the Fermi surface scattering elastically off the aerogel. Finally, the left-hand side of the linearized transport equation provides the driving terms that determine the particular solution for the nonequilibrium distribution functions. The driving terms which are even and odd under  $t_1 \rightarrow -t_1$  are

$$L^{(\pm)}(t_1) = \frac{1}{T} n_0(t_1) (1 - n_0(t_1)) \mathbf{v}_{\mathbf{p}_1} \cdot \left( \frac{\nabla \mu}{\nabla T} \right). \quad (58)$$

We simplify the even and odd components of the transport

equation by an additional transformation of the distribution function,

$$\zeta^{(\pm)}(t) \equiv \frac{1}{\tau_{\text{in}}} \frac{\varphi^{(\pm)}(t)}{2 \cosh(t/2)}. \quad (59)$$

The linearized transport equation with both inelastic and elastic channels included in the collision integral then reduces to the linear integral equations,<sup>35</sup>

$$\begin{aligned} \frac{1}{\cosh(t_1/2)} \begin{pmatrix} 1 \\ t_1 \end{pmatrix} &= \left( t_1^2 + \pi^2 + \frac{2\tau_{\text{in}}}{\tau_{\text{el}}} \right) \zeta^{(\pm)}(t_1) \\ &\mp \lambda^{(\pm)} \int dt_2 \left( \frac{t_1 - t_2}{\sinh((t_1 - t_2)/2)} \right) \zeta^{(\pm)}(t_2), \end{aligned} \quad (60)$$

Physical solutions for  $\zeta^{(\pm)}$  are non-vanishing only in the low-energy region near the Fermi level, i.e.  $|t| \ll 1$ . Thus, we

can Fourier transform,

$$\tilde{\zeta}^{(\pm)}(z) \equiv \int_{-\infty}^{+\infty} dt e^{-izt} \zeta^{(\pm)}(t), \quad (61)$$

and convert the integral equation for  $\zeta^{(\pm)}(t)$  into a linear differential equation for  $\tilde{\zeta}^{(\pm)}(z)$ ,

$$\begin{aligned} \left( \frac{\partial^2}{\partial z^2} - \pi^2 \gamma^2 \right) \tilde{\zeta}^{(\pm)}(z) \mp 2\pi^2 \lambda^{(\pm)} \text{sech}^2(\pi z) \tilde{\zeta}^{(\pm)}(z) \\ = -2\pi \text{sech}(\pi z) \begin{pmatrix} 1 \\ -i\pi \tanh(\pi z) \end{pmatrix}, \end{aligned} \quad (62)$$

where

$$\gamma \equiv \sqrt{1 + \frac{2}{\pi^2} \frac{\tau_{\text{in}}}{\tau_{\text{el}}}}. \quad (63)$$

We cast this differential equation into standard form defined on the domain  $x \in [-1, 1]$  with the transformation,

$$\tanh(\pi z) = x, \quad (64)$$

$$\tilde{\zeta}^{(\pm)}(z) = \mathcal{Z}^{(\pm)}(x), \quad (65)$$

and the differential operator,

$$\mathcal{D}[f] \equiv \frac{d}{dx} \left( (1-x^2) \frac{df}{dx} \right) - \frac{\gamma^2}{(1-x^2)} f. \quad (66)$$

Thus, the nonequilibrium distribution function is obtained as the solution of an inhomogeneous linear differential equation,

$$\mathcal{D}[\mathcal{Z}^{(\pm)}] \mp 2\lambda^{(\pm)} \mathcal{Z}^{(\pm)} = R^{(\pm)}(x), \quad (67)$$

where

$$R^{(\pm)} = \frac{1}{\sqrt{1-x^2}} \begin{pmatrix} -2/\pi \\ +2ix \end{pmatrix}. \quad (68)$$

### G. Thermal Conductivity

The heat current for example can be expressed in terms of a particular solution of Eq. (67),

$$\begin{aligned} \mathbf{j}_q \simeq 2N_f \int \frac{d\Omega_{\hat{\mathbf{p}}}}{4\pi} \int d\xi_{\mathbf{p}} (v_f \hat{\mathbf{p}} \xi_{\mathbf{p}}/T) \\ \times n_0(\xi_{\mathbf{p}}) (1 - n_0(\xi_{\mathbf{p}})) \psi_{\mathbf{p}}(\xi_{\mathbf{p}}). \end{aligned} \quad (69)$$

Carrying out the transformation from  $\psi_{\mathbf{p}}(\xi_{\mathbf{p}}) \rightarrow \mathcal{Z}(x)$  we obtain the following expression for the thermal conductivity,

$$\kappa = \frac{1}{3} (\bar{c}_v v_f) (v_f \tau_{\text{in}}) S_{\kappa}(T), \quad (70)$$

where

$$S_{\kappa}(T) \equiv \frac{3}{4\pi^2} \int_{-1}^{+1} dx R^{(-)}(x) \mathcal{Z}^{(-)}(x). \quad (71)$$

The particular solution for  $\mathcal{Z}^{(-)}$  is obtained as an expansion,

$$\mathcal{Z}^{(-)} = \sum_n \mathcal{A}_n \phi_n(x), \quad (72)$$

in the complete set of orthonormal eigenfunctions,  $\{\phi_n(x)\}$ , of the homogeneous differential equation,

$$\mathcal{D}[\phi_n] + 2\alpha_n \phi_n = 0, \quad (73)$$

where  $\alpha_n$  is the eigenvalue associated with the eigenfunction,  $\phi_n(x)$ . The coefficients,  $\{\mathcal{A}_n\}$ , are determined from Eqs. (67), (68) and (73) and the orthogonality condition,

$$\int_{-1}^{+1} dx \phi_n^*(x) \phi_n(x) = \delta_{n'n}. \quad (74)$$

In particular,

$$\mathcal{A}_n = \frac{c_n}{\lambda_{\kappa} - \alpha_n}. \quad (75)$$

where

$$c_n = \int_{-1}^{+1} dx \phi_n^*(x) R^{(-)}(x), \quad (76)$$

is the overlap of the  $n^{\text{th}}$  eigenfunction with the driving term in the transport equation. Also, we set  $\lambda^{(-)} \equiv \lambda_{\kappa}$  above and hereafter. The same term appears in the kernel of the heat current. Thus, the thermal conductivity, in particular,  $S_{\kappa}(T)$ , is determined by the weighted sum over the eigenvalue spectrum,

$$S_{\kappa}(T) = \frac{3}{8\pi^2} \sum_n \frac{|c_n|^2}{\alpha_n - \lambda_{\kappa}}, \quad (77)$$

### H. Pure Fermi-Liquid

For pure  $^3\text{He}$  ( $\tau_{\text{el}} \rightarrow \infty$ ) Eq. (73) reduces to the differential equation for the associated Legendre functions,<sup>35,37</sup>

$$(1-x^2) \frac{d^2 \phi_n}{dx^2} - 2x \frac{d\phi_n}{dx} \left( 2\alpha_n - \frac{1}{(1-x^2)} \right) \phi_n = 0. \quad (78)$$

The bounded, odd-parity solutions, relevant to heat transport, on the domain  $x \in [-1, +1]$ , are the associated Legendre polynomials,  $P_n^1(x)$  with eigenvalues,  $2\alpha_n = n(n+1)$  for  $n = 1, 2, 3, \dots$ . The standard orthogonality relation for the polynomials is<sup>2</sup>

$$\int_{-1}^{+1} dx P_n^1(x)^* P_{n'}^1(x) = \frac{2n(n+1)}{2n+1} \delta_{nn'}, \quad n \geq 1. \quad (79)$$

The evaluation of the overlap integrals leads to the solution for the thermal conductivity (Eq. (2)) obtained by Brooker



and Sykes,<sup>11,37</sup> and independently by Jensen et al.<sup>20</sup>, with transport time  $\tau_\kappa = \tau_{\text{in}} S_\kappa^\infty$ , where

$$S_\kappa^\infty = \frac{6}{\pi^2} \sum_{m \geq 2}^{\text{even}} \left( \frac{2m+1}{[m(m+1) - 2\lambda_\kappa]m(m+1)} \right), \quad (80)$$

which depends on the angular average of the scattering amplitude via  $\lambda_\kappa$  and is independent of temperature. Thus, the thermal conductivity diverges as  $\kappa \propto 1/T$  as  $T \rightarrow 0$  because the number of thermal excitations, the heat capacity and the number of final states for binary collisions are all vanishing as  $T$ . Note that  $\lambda_\kappa = \langle W(1 + 2\cos\theta) \rangle / \langle W \rangle$  is a measure of the relative importance of forward vs. backscattering, and is restricted to the domain,  $-1 < \lambda_\kappa < 3$ . The resulting spectral sum,  $S_\kappa^\infty$ , is finite since  $\lambda_\kappa < 3$ . However, at any fixed temperature  $\kappa$  increases dramatically for quasiparticle scattering that is predominantly in the forward direction, i.e. for  $\lambda_\kappa \rightarrow 3$ . Note also that  $S_\kappa^\infty \rightarrow \frac{5}{6\pi^2} \frac{1}{1 - \frac{1}{3}\lambda_\kappa}$  in this limit.

### I. Exact Solution

Here we extend the exact solution for pure  $^3\text{He}$ <sup>11,20</sup> to that of  $^3\text{He}$  in aerogel described by the two-channel collision integral for binary quasiparticle collisions and quasiparticle-aerogel scattering. Bennett and Rice extended the analysis of Refs. 11,20 to collisional scattering of s- and d-electrons combined with electron-impurity scattering.<sup>10</sup> Their results for the electrical and thermal conductivity are expressed as a sum over weighted integrals of products of Gegenbauer polynomials. Our analysis also starts from a two-channel extension of the integral equation of Refs. 11,20, i.e. Eq. (60). The results presented below are a closed form analytic solution to the linearized Boltzmann equation and thermal conductivity, and an exact perturbation theory result for the inelastic corrections to the elastic limit which is used to develop a very accurate approximate solution for the thermal conductivity that is valid for all temperatures (above  $T_c$ ), pressures and aerogel densities, and is fast and easy to evaluate.

Elastic scattering by the aerogel modifies the form of the eigenfunctions for the nonequilibrium distribution function, and leads to an eigenvalue spectrum that varies strongly with temperature. The key parameter is the structure constant ( $\gamma$ ) in Eqs. (62) and (63) in the differential equation for the distribution function. The temperature dependence is conveniently exhibited by scaling Eq. (63) in terms of the cross-over temperature,  $T_*$ , defined in Eq. (5),

$$\gamma = \sqrt{1 + \frac{2}{\pi^2} \left( \frac{T_*}{T} \right)^2}. \quad (81)$$

The eigenfunctions of Eq. (73) for any  $\gamma > 1$  must be bounded on the interval  $[-1, +1]$ . The singular points at  $x = \pm 1$  have indicial equations with one physically allowed

solution in the neighborhood of the singular point; in particular, since  $\gamma > 1$  we select the physical solutions which must behave as

$$\phi_n \sim (1-x)^{\gamma/2}, \quad x \sim +1 \quad (82)$$

$$\phi_n \sim (1+x)^{\gamma/2}, \quad x \sim -1. \quad (83)$$

Thus, we extract the behavior near the singular points and express

$$\phi_n(x) = (1-x^2)^{\gamma/2} g_n(x), \quad (84)$$

where  $g_n(x)$  is analytic on the domain  $[-1, +1]$ , and governed by the differential equation,

$$(1-x^2) \frac{d^2 g_n}{dx^2} - 2(\gamma+1)x \frac{dg_n}{dx} + [2\alpha_n - \gamma(\gamma+1)]g_n = 0. \quad (85)$$

Analytic solutions on the finite domain can be represented as a Taylor expansion about  $x = 0$ ,

$$g_n(x) = \sum_{m=0}^{\infty} G_m x^m. \quad (86)$$

The differential equation determines the recurrence formula for the coefficients,

$$G_{m+2} = \frac{N_m}{(m+2)(m+1)} G_m, \quad (87)$$

$$N_m = [m(m-1) + 2m(\gamma+1) + \{\gamma(\gamma+1) - 2\alpha_m\}].$$

Thus, the solutions break up into even and odd parity solutions depending on the coefficients  $G_0$  and  $G_1$ . For even parity solutions, we set  $G_0 \neq 0$  and generate the solutions from the recurrence relation:

$$G_m = \frac{N_0 N_2 \dots N_{m-2}}{m!} G_0, \quad m = 2, 4, \dots \quad (88)$$

Similarly, for the odd-parity solutions we start from  $G_1 \neq 0$  and find

$$G_m = \frac{N_1 N_3 \dots N_m}{(m+2)!} G_1, \quad m = 3, 5, \dots \quad (89)$$

In either case

$$\lim_{m \rightarrow \infty} \frac{G_{m+2}}{G_m} \rightarrow 1. \quad (90)$$

Thus, the series solution diverges at  $|x| = 1$  *unless* the expansion truncates at a finite value of  $m$ . This restricts the physical solutions for  $g_n(x)$  to a set of polynomials, and an eigenvalue spectrum determined by the condition:

$$G_{n+2} = 0 \rightsquigarrow N_n = 0. \quad (91)$$

Expressing the eigenvalue as  $2\alpha_n = \epsilon_n(\epsilon_n + 1)$ , we obtain

$$\epsilon_n = \gamma + n, \quad n = 0, 2, 4, \dots \quad (n = 1, 3, 5, \dots), \quad (92)$$

for even (odd) parity solutions. The corresponding eigenfunctions are

$$\phi_n(x) = (1 - x^2)^{\gamma/2} \sum_m^n G_m^{(n)} x^m, \quad (93)$$

with the summation over even (odd) integers for even (odd) parity eigenfunctions. The coefficients can be expressed in terms of Gamma functions. In particular, for the odd-parity eigenfunctions, which are relevant for computing the thermal conductivity,

$$C_m^{(n)} \equiv G_m^{(n)} / G_1^{(n)} = (-1)^{(m-1)/2} \frac{2^{m-1}}{m!} \times \frac{\Gamma(\frac{n}{2} + \frac{1}{2})}{\Gamma(\frac{n-m}{2} + 1)} \frac{\Gamma(\gamma + \frac{n}{2} + 1 + \frac{m-1}{2})}{\Gamma(\gamma + \frac{n}{2} + 1)}. \quad (94)$$

Coefficient  $G_1^{(n)}$  is fixed by the normalization of  $\phi_n(x)$ ,

$$|G_1^{(n)}|^2 = \left[ \sum_{m=1}^n \sum_{p=1}^n C_m^{(n)} C_p^{(n)} \mathcal{B}(\gamma + 1, \frac{m+p+1}{2}) \right]^{-1}, \quad (95)$$

and  $\mathcal{B}(x, y) = \Gamma(x)\Gamma(y)/\Gamma(x+y)$  is the Beta function.<sup>2</sup>

We can now evaluate the spectral sum in Eq. (77) to obtain an exact solution for the thermal conductivity. In particular,

$$S_\kappa(T) = \frac{3}{\pi^2} \sum_{\ell=1}^{\infty} \left[ \frac{1}{(\gamma + 2\ell)(\gamma + 2\ell - 1) - 2\lambda_\kappa} \right] \frac{\left| \sum_{p=1}^{\ell} C_p^{\ell} \mathcal{B}(\frac{\gamma+1}{2}, p + \frac{1}{2}) \right|^2}{\sum_{p=1}^{\ell} \sum_{q=1}^{\ell} C_p^{\ell} C_q^{\ell} \mathcal{B}(\gamma + 1, p + q - \frac{1}{2})}, \quad (96)$$

where

$$C_p^{\ell} \equiv C_{2p-1}^{2\ell-1} = (-4)^{p-1} \frac{\Gamma(\gamma + \ell + p - \frac{1}{2})}{\Gamma(2p)\Gamma(\ell - p + 1)}. \quad (97)$$

Although Eq. (96) provides us with an exact, closed form solution for the thermal conductivity over the full temperature and pressure range,  $T_c \leq T \ll T_f$ , the sums defining  $S_\kappa(T)$  involve ratios of Gamma functions. Thus, care must be taken in evaluating these functions even for moderate values of their arguments. This is particularly true in the low-temperature limit,  $T \ll T_\star$ , since the scaling parameter,  $\gamma$  becomes large. However, the limit  $T \ll T_\star$  can also be evaluated using perturbation theory.

## J. Perturbation Theory

At temperatures  $T \ll T_\star$  inelastic quasiparticle collisions are relatively infrequent compared to elastic collisions off the aerogel. Thus, the inelastic collision integral in Eq. (34) is of order

$$\frac{\delta I^{\text{in}}}{\delta I^{\text{el}}} \sim \frac{\tau_{\text{el}}}{\tau_{\text{in}}} \sim \left( \frac{T}{T_\star} \right)^2 \equiv \delta \ll 1, \quad (98)$$

and we can formally expand the integral equation and the deviation from local equilibrium in the small parameter  $\delta$ ,

$$\delta \bar{n}_{p_i} = \delta \bar{n}_{p_i}^{(0)} + \delta \bar{n}_{p_i}^{(1)} + \dots \quad (99)$$

The perturbation expansion through first order becomes,

$$L(\xi_{p_1}, \hat{\mathbf{p}}_1) = \delta I_{p_1}^{\text{el}} [\delta \bar{n}_p^{(0)}], \quad (100)$$

$$0 = \delta I_{p_1}^{\text{in}} [\delta \bar{n}_p^{(0)}] + \delta I_{p_1}^{\text{el}} [\delta \bar{n}_p^{(1)}]. \quad (101)$$

where  $L(\xi_{p_1}, \hat{\mathbf{p}}_1)$  represents the driving term on the left side of Eq. (34). For heat transport the zeroth-order solution of Eq. (100) is simply the distribution in the elastic scattering limit,

$$\delta \bar{n}_{p_i}^{(0)} = \left( \frac{\partial n_0}{\partial \xi_{p_i}} \right) \left( \frac{\xi_{p_i}}{T} \right) (\mathbf{v}_{p_i} \cdot \nabla T) \tau_{\text{el}}, \quad (102)$$

and now provides the driving term for the first order correction in Eq. (101). This equation has the same integral kernel as that of Eq. (100) and so we can express the first-order correction in terms of an inelastic correction to the scattering time,

$$\delta \bar{n}_{p_i}^{(1)} = \left( \frac{\partial n_0}{\partial \xi_{p_i}} \right) \left( \frac{\xi_{p_i}}{T} \right) (\mathbf{v}_{p_i} \cdot \nabla T) \tau_1(\xi_{p_i}), \quad (103)$$

where  $\tau_1$  is the first-order correction to the mean scattering time,  $\tau_{\text{el}}$ . This distribution function gives the first order elastic collision integral,

$$\delta I_{p_1}^{\text{el}} [\delta \bar{n}_p^{(1)}] = - \left( \frac{\partial n_0}{\partial \xi_{p_1}} \right) \left( \frac{\xi_{p_1}}{T} \right) (\mathbf{v}_{p_1} \cdot \nabla T) \frac{\tau_1}{\tau_{\text{el}}}. \quad (104)$$

The solution of the Eq. (101) can then be expressed in terms of  $\tau_1$ . The analysis of the inelastic collision integral, evalu-

ated with the zeroth order nonequilibrium distribution function,  $\delta\bar{n}_{p_i}^{(0)}$ , leads to

$$\tau_1 = -\frac{\tau_{\text{el}}^2}{\tau_{\text{in}}} (n_0(t_1)(1 - n_0(t_1)) t_1)^{-1} \times \left[ n_0(t_1) I_1 t_1 + \lambda_\kappa n_0(t_1) J_1 \right], \quad (105)$$

where  $I_1 = I(\xi_1)/T^2$ , with  $I(\xi_1)$  given by Eq. 54, and

$$J_1 = \frac{1}{T^3} \int d\xi_2 \xi_2 n_0(\xi_2) K(\xi_1 + \xi_2) = -\frac{1}{6} (\pi^2 + t^2) t_1 (1 - n_0(t_1)), \quad (106)$$

with  $K(\xi)$  defined by Eq. 53. The resulting first-order correction for the collision time reduces to

$$\tau_1 = -\frac{1}{2} \frac{\tau_{\text{el}}^2}{\tau_{\text{in}}} (\pi^2 + t_1^2) \left( 1 - \frac{1}{3} \lambda_\kappa \right), \quad (107)$$

which vanishes in the “ballistic limit” for inelastic collisions,  $\lambda_\kappa \rightarrow 3$ .

The first order correction to the thermal conductivity is calculated by evaluating Eq. (21) with the first-order correction,  $\delta\bar{n}_p^{(1)}$ . Writing  $\mathbf{j}_q^{(1)} = -\delta\kappa \nabla T$ , we obtain,

$$\delta\kappa = \frac{2}{3} N_f v_f^2 T \int_{-\infty}^{+\infty} dt \frac{t^2}{4 \cosh^2(t/2)} \tau_1(t). \quad (108)$$

After the integration over  $\tau_1(t)$ , and scaling to the elastic limit for the thermal conductivity given in Eq. (33), we obtain,

$$\frac{\delta\kappa}{\kappa_{\text{el}}} = -\frac{6}{5} \pi^2 \left( 1 - \frac{1}{3} \lambda_\kappa \right) \left( \frac{\tau_{\text{el}}}{\tau_{\text{in}}} \right). \quad (109)$$

### III. RESULTS

Theoretical models for the quasiparticle collision probability,  $W(\theta, \phi)$ , for pure  $^3\text{He}$  have been proposed by a number of authors.<sup>13,24,26,33</sup> We use an extended version of the *s-p model* introduced by Dy and Pethick<sup>13</sup>, described as the *spd model* in Sec. V. In Fig. 2 we compare the results for the thermal transport scattering time,  $\tau_\kappa T^2$ , for pure  $^3\text{He}$  calculated in the *spd model* with the Landau parameters taken from Refs. 17,19 and the limiting low-temperature thermal conductivity measurements from Greywall (Table II of Ref. 16). The theoretical and experimental results are in agreement over the pressure range,  $p = 0 - 25$  bar provided the forward-scattering sum rule (FSSR) is enforced (see Eq. (165) in the Appendix). Above 25 bar there are deviations  $0\% \leq \delta\tau_\kappa/\tau_\kappa \leq 14\%$  indicating the role of additional scattering not described by the *spd model*. Note in particular that the dimensionless scattering parameter,  $\lambda_\kappa$ , is nearly constant over the entire pressure range, i.e.  $1.0 \lesssim \lambda_\kappa \lesssim 1.3$ .

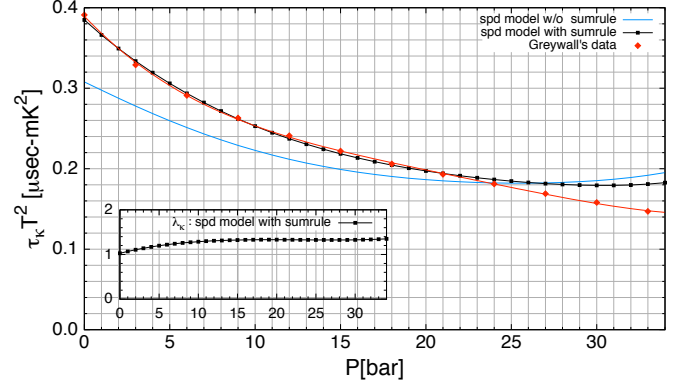


FIG. 2: Pressure dependence of the low-temperature limit of the thermal transport time  $\tau_\kappa T^2$  for pure  $^3\text{He}$ . The red  $\blacklozenge$  are the data from Ref. 16. The blue — is the *spd model* without enforcing the FSSR, and the [black ■] are the *spd model* with the FSSR enforced. Inset:  $\lambda_\kappa$  calculated in the *spd model* with the FSSR enforced.

#### A. Results for $^3\text{He}$ -aerogel

Theoretical results for heat transport in  $^3\text{He}$ -aerogel based on the two-channel solution for the thermal conductivity are shown in Fig. 3. In addition to the *mfp* describing the aerogel, the input data for bulk  $^3\text{He}$  used to generate these results are density ( $n$ ), effective mass ( $m^*$ ), Fermi velocity ( $v_f$ ) and the Fermi liquid parameters ( $F_l^{s,a}$ ) for  $l \leq 2$ , all of which are taken from the database provided in Ref. 17 and 19. The Fermi-liquid parameters are used to construct the inelastic scattering rate using the *spd model* as described in the Appendix (Sec. V).

The cross-over from the high-temperature regime dominated by inelastic quasiparticle collisions to the low-temperature regime dominated by elastic scattering by the disordered medium occurs over a fairly broad temperature range for dilute aerogels with long *mfp*. The elastic regime below  $T \simeq 5 - 10$  mK is well described by  $\kappa = \kappa_{\text{el}} + \mathcal{O}(T^3)$ , with  $\kappa_{\text{el}}$  given by Eq. (33). The pressure dependence of the slope of  $\kappa_{\text{el}}(T)$ , while not visible in Fig. 3, is shown clearly in Fig. 4. Note that  $\lim_{T \rightarrow 0} \kappa/T$  can provide a determination of the elastic *mfp* for the aerogel.

Figure 4 for  $\kappa/T$  highlights the deviations in the thermal conductivity from the elastic limit limit even at temperatures of order a few milli-Kelvin. Similarly, in the high temperature limit the product,  $\kappa T$ , approaches the bulk  $^3\text{He}$  limit determined by inelastic scattering. Significant deviations from the pure  $^3\text{He}$  limit are shown in Fig. 5 over a wide range of temperatures above  $T_*$ .

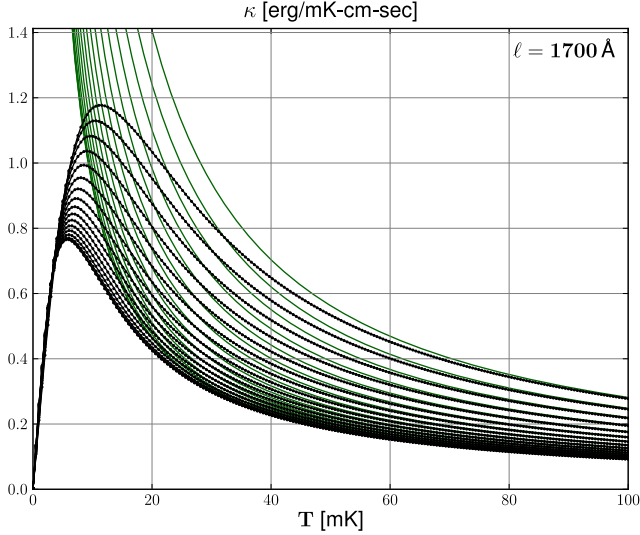


FIG. 3: Theoretical results for the thermal conductivity of  $^3\text{He}$ -aerogel vs.  $T$  and  $p$  for an elastic  $mfp$  of  $\ell = 1700 \text{ \AA}$  are shown in **black**  $-\bullet-$ ; results for pure  $^3\text{He}$  are shown as **green lines**. The pressure ranges from  $p = 0 - 32$  bar in steps of 2 bar starting with the the upper curve at  $p = 0$  bar.

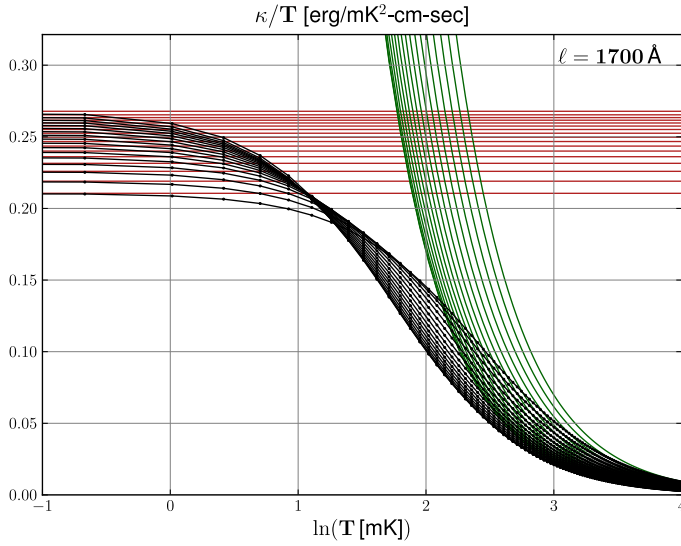


FIG. 4:  $\kappa/T$  vs.  $\ln(T[\text{mK}])$  and  $p[\text{bar}]$ . The inputs and labels are the as Fig. 3. The slopes for the elastic limit,  $\kappa_{\text{el}}/T$ , are shown in **darkred**  $-$ .

## B. Comparison with Experiments

Barker *et.al*<sup>7</sup> reported results for the thermal conductivity of  $^3\text{He}$  in 98% at aerogel of  $\kappa = 7.2 \text{ mW/mK}$  at  $p = 32.4 \text{ bar}$  and  $T = 2.20 \text{ mK}$ . They also added two monolayers for  $^4\text{He}$  which displaces the solid  $^3\text{He}$  coating the silica aerogel strands, and measured a slight *increase* in the thermal

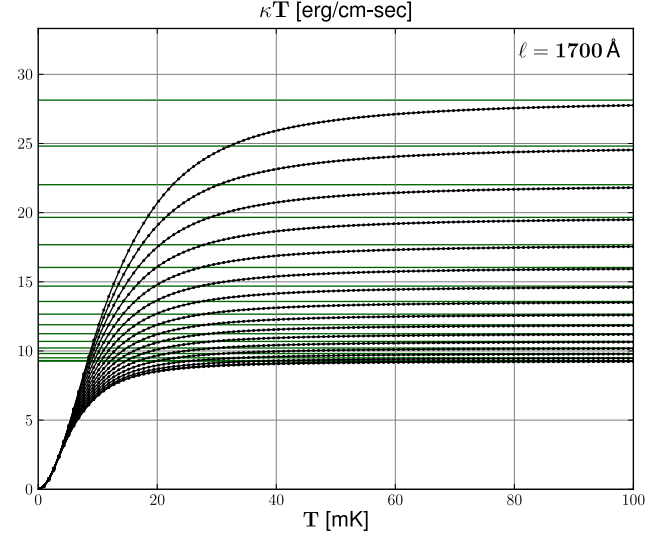


FIG. 5:  $\kappa T$  vs.  $T[\text{mK}]$  and  $p[\text{bar}]$ . The inputs and labels are the same as those of Fig. 3. Note that results for  $\kappa T$  for bulk  $^3\text{He}$  are shown as **darkgreen**  $-$ .

conductivity, i.e.  $\kappa = 7.7 \text{ mW/mK}$  at  $T = 2.22 \text{ mK}$ . Comparison of these two data points with the theoretical predictions for this pressure are shown in Fig. 6.

If the difference in the  $mfp$  with and without the  $^4\text{He}$  is attributable to spin-exchange scattering of itinerant  $^3\text{He}$  spins by the localized solid  $^3\text{He}$  spins,<sup>6,34</sup> then we can estimate the contribution to the scattering rate from indirect spin-exchange scattering to be,

$$\frac{1}{\tau_{\text{spin}}} = v_f \left( \frac{1}{\ell_{^3\text{He}}} - \frac{1}{\ell_{^3\text{He}+^4\text{He}}} \right), \quad (110)$$

and thus a mean time for spin-exchange scattering of  $\tau_{\text{spin}} \simeq 0.15 \mu\text{sec}$ , i.e. several orders of magnitude longer than the mean time for elastic scattering off the aerogel strands,  $\tau_{\text{el}} \simeq \ell_{^3\text{He}+^4\text{He}}/v_f \simeq 8.6 \text{ ns}$ . For scattering off a random distribution of  $N_s$  localized spins via a Kondo interaction,

$$u = - \sum_{i=1}^{N_s} (J_{\text{ind}}/n) \mathbf{S}_i \cdot \boldsymbol{\sigma} \delta(\mathbf{r} - \mathbf{R}_i), \quad (111)$$

the Born approximation implies an additional contribution to the scattering rate,

$$\hbar/\tau_{\text{spin}} = \frac{4\pi n_s}{N_f} (J_{\text{ind}}/n)^2 S(S+1). \quad (112)$$

Thus, we estimate the indirect exchange interaction to be

$$J_{\text{ind}} = E_f \left[ \left( \frac{4}{9\pi} \right) \left( \frac{\hbar/\tau_{\text{spin}}}{E_f} \right) \left( \frac{n}{n_s} \right) \right]^{1/2} \simeq 0.5 \text{ mK/spin}, \quad (113)$$

which is in agreement with the order of magnitude estimate for  $J_{\text{ind}}$  inferred from the absence of a low-field  $A_1 - A_2$  transition in  $^3\text{He}$ -aerogel.<sup>34</sup>

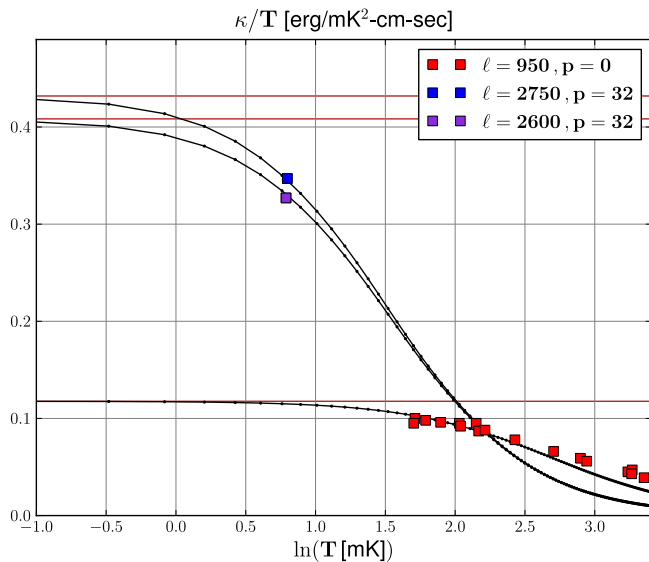


FIG. 6: Comparison  $\kappa/T$  vs.  $\ln(T[\text{mK}])$  with experiments. Data shown as  $\blacksquare$  is from the Lancaster group for a 98% aerogel and a pressure of  $p \simeq 0$  bar.<sup>30</sup> Data shown as  $\blacksquare$  (purple) is from the Stanford group with two monolayers of  $^4\text{He}$  coating (without  $^4\text{He}$ ) the silica strands at high pressure ( $p = 32.4$  bar), also for 98% aerogel but grown in a different laboratory. The  $\text{---}$  show  $\lim_{T \rightarrow 0} \kappa/T$ .

### C. Scaling Function

The exact solution for the thermal conductivity in the two-channel scattering theory for  $^3\text{He}$ -aerogel can be expressed in terms of a scaling function. Normalizing  $\kappa$  by the thermal conductivity in the elastic limit,  $\kappa_{\text{el}}$ , from Eq. (33) gives,

$$\frac{\kappa}{\kappa_{\text{el}}} = \frac{\tau_{\text{in}}}{\tau_{\text{el}}} \times S_{\kappa}(T) \equiv F(T/T^*, \lambda_{\kappa}). \quad (114)$$

Note that  $\tau_{\text{el}}/\tau_{\text{in}} \equiv (T/T^*)^2$ , and that  $S_{\kappa}(T)$  calculated from Eq. (77) [Eq. (96) in Sec. III] provides the *exact* scaling function,  $F(x, \lambda)$ , since  $S_{\kappa}(T)$  depends only on  $x = T/T^*$  and the scattering ratio,  $-1 < \lambda_{\kappa} < 3$ . Thus, the test of the two-channel transport theory would be to demonstrate that the thermal conductivity of  $^3\text{He}$ -aerogel obeys the scaling behavior over the full temperature and pressure range of the normal state, and a broad range of aerogel density and  $mfp$ .

The exact solution for  $\kappa/\kappa_{\text{el}} \times (T/T^*) \equiv x F(x, \lambda_{\kappa})$  is shown in Fig. (7). The calculation of spectral sum,  $S_{\kappa}(T)$ , was carried out using arbitrary-precision floating point arithmetic in order to evaluate the ratios of the Gamma functions or large arguments that enter Eq. (96) with sufficient precision to obtain accurate results for the triple sum that defines  $S_{\kappa}(T)$ . In particular, the points labeled “exact” in Fig. (7) were obtained with the floating point precision set at 55 digits and

The Lancaster group also reports results for the low-temperature (i.e.  $T \ll T^*$ ) thermal conductivity of normal  $^3\text{He}$ -aerogel at low pressures, for aerogels with porosities of 95% and 98%.<sup>30</sup> Results for  $\varrho = 98\%$  reported in Ref. 30 yield a much smaller  $mfp$ ,  $\ell = 950 \text{ \AA}$ , than the Stanford data, suggesting significant differences in aerogels of the same density prepared under different growth conditions. Note that the authors of Ref. 30 attribute the deviations from the theoretical curve onset near  $T \simeq 20 \text{ mK}$  ( $\ln(T[\text{mK}]) \simeq 3$ ) to Kapitza boundary conductance through the experimental cell walls.

Although these results provide estimates for the aerogel  $mfp$  they do not provide a test of the theory. Measurements of the thermal conductivity over the full temperature and pressure range of normal  $^3\text{He}$ -aerogel should provide a strong test of the two-channel theory based on homogeneous disorder since we have an exact solution for the thermal conductivity in this model. Conversely, if significant deviations from the theoretical predictions are observed they could indicate new physics associated scattering and transport of fermionic excitations in a correlated random medium.

each sum was cutoff after 30 terms were computed. One can obtain reasonably good results with a lower precision setting for the floating point arithmetic, but double precision on a 32-bit machine limits the accuracy of the results, particularly in the limit  $T < T^*$ .

Also shown in Fig. (7) are calculations of the scaling function based on an approximate analytic formula that is numerically fast and easy to evaluate. The approximate scaling function is constructed from the asymptotic limits for  $S_{\kappa}(T)$  for  $T \gg T^*$  and  $T \rightarrow 0$ , as well as the leading order perturbative result for  $T \ll T^*$ , as described below.

The limiting behavior for the exact scaling function is known from the asymptotic limit,  $x \gg 1$ , and perturbation theory about  $x = 0$ . In particular,

$$F(x, \lambda_{\kappa}) = \begin{cases} 1 - \frac{6}{5}\pi^2(1 - \frac{1}{3}\lambda_{\kappa})x^2 & , x \ll 1 \\ \frac{1}{x^2} S_{\kappa}^{\infty} & , x \gg 1, \end{cases} \quad (115)$$

where  $S_{\kappa}^{\infty}$  is given by Eq. (80).

The most common approximate solution for multi-channel scattering is based *Matthiessen's Rule*, which in this context



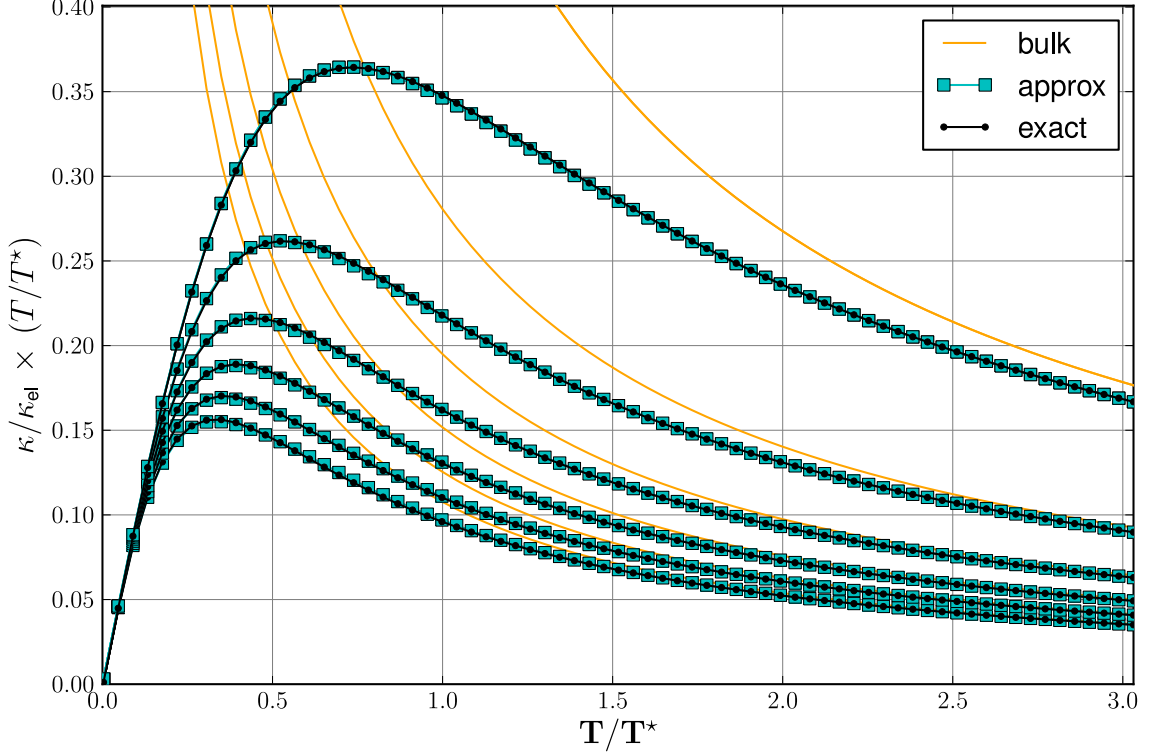


FIG. 7: Scaling function for the thermal conductivity plotted as  $x F(x, \lambda_\kappa) \equiv \kappa/\kappa_{\text{el}} \times (T/T_\star)$  as a function of  $x = T/T_\star$  for  $\lambda_\kappa = 0.0, 0.5, 1.0, 1.5, 2.0, 2.5$ , starting from the lowest to the highest curve, respectively. The exact results based on Eqs. 81,97 and 96 are shown as the **Black**  $-\bullet-$ , the **Cyan**  $\blacksquare$  are based on the approximate analytic formula given in Eqs. (132, 133, 118 and 127), and the **Orange**  $-$  are the results for pure, bulk  $^3\text{He}$  normalized to the elastic limit for  $^3\text{He}$ -aerogel.

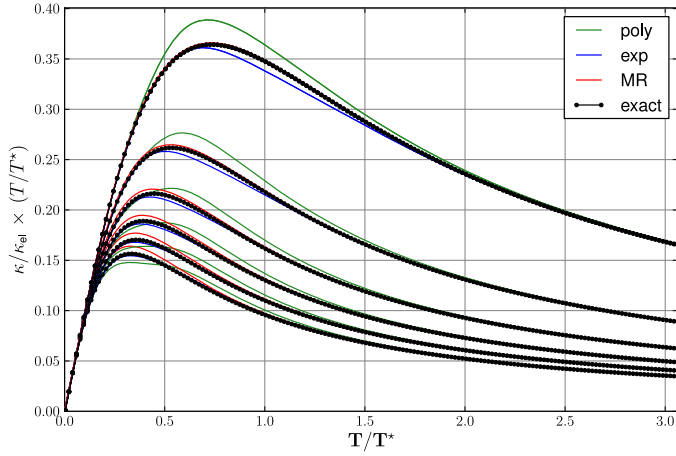


FIG. 8: Comparison of several approximates with the exact scaling function,  $x F(x, \lambda_\kappa)$ , plotted as a function of  $x = T/T_\star$  for  $\lambda_\kappa = 0.0, 0.5, 1.0, 1.5, 2.0, 2.5$ , starting from the lowest to the highest curve, respectively. The exact results are shown in **Black**  $-\bullet-$ , while the approximate scaling functions, labelled as **poly**, **exp** and **MR**, are described in the text.

can be expressed as

$$\frac{1}{\tau_\kappa^{\text{MR}}} = \frac{1}{\tau_{\text{el}}} + \frac{1}{S_\kappa^\infty \tau_{\text{in}}(T)}, \quad (116)$$

i.e. the total transport scattering rate is the sum of independent rates for purely elastic and purely bulk inelastic transport. The resulting expression for the the thermal conductivity, normalized to its value in the elastic limit,

$$\bar{\kappa}^{\text{MR}} = \frac{\tau_\kappa^{\text{MR}}}{\tau_{\text{el}}} \equiv F_{\text{MR}}(T/T_\star, \lambda_\kappa), \quad (117)$$

defines the approximate scaling function,  $F_{\text{MR}}(x, \lambda_\kappa)$  given by,

$$F_{\text{MR}}(x, \lambda_\kappa) = \frac{1}{1 + (S_\kappa^\infty)^{-1} x^2} = \begin{cases} 1 - (S_\kappa^\infty)^{-1} x^2, & x \ll 1 \\ S_\kappa^\infty \frac{1}{x^2}, & x \gg 1. \end{cases} \quad (118)$$

The MR scaling function deviates from the exact result of Eq. (115) for the leading order finite temperature correction. Curiously, the exact result for the leading order correction is equal to that obtained from  $F_{\text{MR}}(x, \lambda_\kappa)$  by approximating  $S_\kappa^\infty$  with just the first term of the sum in Eq. (80). This approximation is very good in the limit of nearly forward scattering. In this limit the inelastic channel leads to large

thermal transport for  $T \gtrsim T_*$ . As a result the MR scaling function gives a very good approximation to the exact scaling function in the limit of large  $\lambda_\kappa$  for all  $x$ . This is shown clearly in Fig. (8). However, the MR scaling function deviates from the exact scaling function when backscattering in the inelastic channel is significant, i.e. for  $\lambda_\kappa \lesssim 1.0$ . These deviations are also clearly visible in Fig. (8).

We can try to improve on the MR scaling function by incorporating the exact perturbative result for  $F(x, \lambda_\kappa)$  for  $x \ll 1$ . We construct an interpolation formula that connects the exact asymptotic limits. A simple extension of Matthiessen's interpolation formula is the two-parameter, rational polynomial function,

$$F_{\text{poly}} = \frac{1}{1+ax^2} + \frac{x^2}{1+bx^4}, \quad (119)$$

which has the limiting forms,

$$F_{\text{poly}} = \begin{cases} 1 - (a-1)x^2, & x \ll 1 \\ \left(\frac{1}{a} + \frac{1}{b}\right) \frac{1}{x^2}, & x \gg 1. \end{cases} \quad (120)$$

We then fix the coefficients from the exact asymptotic limits for  $F(x, \lambda_\kappa)$  in Eq. (115),

$$a = 1 + \frac{6}{5}\pi^2 \left(1 - \frac{1}{3}\lambda_\kappa\right) \quad (121)$$

$$b = \frac{a}{aS_\kappa^\infty - 1}. \quad (122)$$

Although this approximate scaling function works well for the  $x \ll 1$ , it does a poor job in the intermediate and high-temperature region  $x \gtrsim 1$  (green curves in Fig. 8), and is particularly poor for  $\lambda_\kappa \rightarrow 3$ . If we consider the leading order correction to the asymptotic limit  $x \rightarrow \infty$  we obtain

$$F \rightarrow \frac{S_\kappa^\infty}{x^2} + C_4 \frac{1}{x^4} + \mathcal{O}\left(\frac{1}{x^6}\right). \quad (123)$$

For the polynomial approximate we obtain,

$$C_4^{\text{poly}} = -\frac{1}{\left(1 + \frac{6\pi^2}{5}(1 - \lambda_\kappa/3)\right)^2}, \quad (124)$$

while the MR scaling function gives

$$C_4^{\text{MR}} = -(S_\kappa^\infty)^2. \quad (125)$$

Both approximate scaling functions give the correct sign for the leading order correction, however in the limit  $\lambda_\kappa \rightarrow 3$ , where we know the MR scaling function approaches the exact result, we see that  $C_4^{\text{MR}}$  is large and negative,

$$C_4^{\text{MR}} \rightarrow -\left(\frac{5}{6\pi^2}\right)^2 \frac{1}{(1 - \lambda_\kappa/3)^2}, \quad (126)$$

whereas  $C_4^{\text{poly}} \rightarrow -1$ . This discrepancy in  $F_{\text{poly}}$  is traced to the contamination of the temperature region  $x > 1$  by the exact solution that is valid for  $x \ll 1$ .

We might remedy this problem with a two-parameter interpolation that limits the contamination between  $x \ll 1$  and  $x \gg 1$ . In particular, consider the approximate scaling function,

$$F_{\text{exp}} = \frac{1}{2}e^{-2ax^2} + \frac{1}{2}\left(1 - e^{-2b/x^2}\right). \quad (127)$$

For  $x \ll 1$ ,

$$F_{\text{exp}} \xrightarrow{x \ll 1} 1 - ax^2 + \mathcal{O}(x^4). \quad (128)$$

Note that there are only exponentially small corrections to the leading order result for  $x \ll 1$  coming from the terms that are fixed by the asymptotic solution for  $x \gg 1$ . Similarly, for  $x \gg 1$ , the term that is fixed by the exact solution for  $x \ll 1$  is now exponentially small and we obtain,

$$F_{\text{exp}} \xrightarrow{x \gg 1} \frac{b}{x^2} - \frac{b^2}{x^4} + \mathcal{O}\left(\frac{1}{x^6}\right). \quad (129)$$

Using these expansions and the exact leading order asymptotic limits we obtain

$$a = \frac{6\pi^2}{5}(1 - \lambda_\kappa/3) \quad (130)$$

$$b = S_\kappa^\infty. \quad (131)$$

This two-parameter interpolation formula yields a better approximation to the exact scaling function, particularly for  $\lambda_\kappa \lesssim 1$ . However,  $F_{\text{exp}}$  under estimates the maximum in  $x F(x, \lambda_\kappa)$ , and this deviation is enhanced as  $\lambda_\kappa \rightarrow 3$ , as is clear from Fig. (8). The basic result of this analysis is that the MR scaling function,  $F_{\text{MR}}$ , is accurate in the limit of large  $\lambda_\kappa$ , but deviates from exact scaling for  $\lambda_\kappa \lesssim 1$ . By contrast the two-parameter exponential scaling function,  $F_{\text{exp}}$ , is accurate in limit  $\lambda_\kappa < 1$ , but shows increasing errors from exact scaling in the cross-over region,  $x \sim \mathcal{O}(1)$ , for  $1 < \lambda_\kappa < 3$ . This suggests that we combine these two scaling functions into a single scaling function by weighting the respective regions of accurate scaling, i.e.

$$F_{\text{approx}}(x, \lambda_\kappa) = \mathbf{p}(\lambda_\kappa) F_{\text{exp}}(x, \lambda_\kappa) + (1 - \mathbf{p}(\lambda_\kappa)) F_{\text{MR}}(x, \lambda_\kappa), \quad (132)$$

where the weight function  $\mathbf{p}(\lambda_\kappa)$  is chosen on the physical domain,  $-1 < \lambda_\kappa < 3$ , to satisfy,  $\mathbf{p}(-1) = 1$ ,  $\mathbf{p}(+3) = 0$ . Thus, the simplest weight functions which map the physical domain onto the interval  $[0, 1]$  are

$$\mathbf{p}(\lambda_\kappa) = \left(\frac{1 + \lambda_\kappa}{4}\right)^s. \quad (133)$$

The quadratic weight function, i.e.  $s = 2$ , leads to remarkably good agreement with the exact scaling function for the entire domain of  $\lambda_\kappa$  and reduced temperature,  $x = T/T_*$ . This comparison is shown in Fig. (7). Note that the maximum deviation for any of the computed values is less than 0.6%, and careful examination shows that these small errors occur near the maxima of  $x F(x, \lambda_\kappa)$ . Thus, the main result here is that Eqs. 118, 127, 132 and 133 provide numerically fast and accurate formulas for calculating the thermal conductivity over the full temperature and pressure range within the two-channel scattering theory for normal  $^3\text{He}$ -aerogel.

### D. Scaling for $^3\text{He}$ -aerogel

The analysis of the pressure dependence of the thermal conductivity of pure  $^3\text{He}$  based on the spd scattering amplitude described in Sec. III and App. V implies that the thermal transport scattering parameter is nearly pressure independent, i.e.  $\lambda_\kappa \simeq 1.3$  for  $5 \text{ bar} \lesssim p \leq 34 \text{ bar}$  with a smooth drop to  $\lambda_\kappa \simeq 1.0$  as pressures between 5 and 0 bar (see inset of Fig. 2).

Pressure independence of the scattering parameter,  $\lambda_\kappa$ , implies that the thermal conductivity for *all temperatures* above the superfluid transition, *all pressures* and *all elastic mean-free paths* should collapse to a single scaling function when normalized to its value in the elastic scattering limit, i.e.  $\lim_{T \rightarrow 0} \kappa = \kappa_{\text{el}}$  given in Eq. (33). Thus, for  $^3\text{He}$ -aerogel we expect that thermal conductivity for all  $T$ ,  $p$  and  $\ell$  to collapse to the narrow band of scaling functions shown in Fig. 9. A complete set of measurements of the thermal conductivity of  $^3\text{He}$ -aerogel for all  $T$ ,  $p$  and a wide range of aerogel  $mfp$  would provide a strong test of this theory, particularly the assumption of uncorrelated disorder described by a single  $mfp$ .

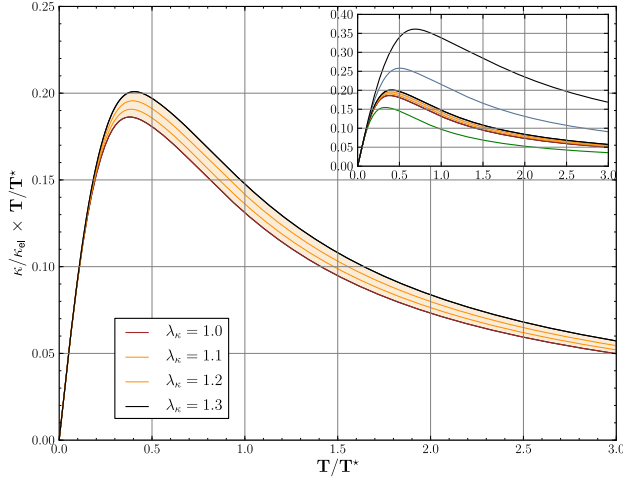


FIG. 9: Scaling of the thermal conductivity with  $T/T_*$  for  $^3\text{He}$ -aerogel for the physical range:  $1.0 \leq \lambda_\kappa \leq 1.3$ . Inset: Scaling function for a much larger parameter range of transport scattering parameters, including  $\lambda_\kappa = 0.0, 2.0, 2.5$ , in addition to the physical range.

### IV. SUMMARY

Liquid  $^3\text{He}$  impregnated into silica aerogel is a model system for investigating the effects of quenched disorder on the properties of a strongly correlated Fermi liquid. In the normal Fermi liquid the transport of heat, mass and spin by fermionic excitations exhibits cross-over behavior from a high temperature regime, where inelastic scattering dom-

inates, to a low temperature regime dominated by elastic scattering off the aerogel. The exact solution to the two-channel Boltzmann-Landau transport equation reported here provides quantitative predictions for heat transport in liquid  $^3\text{He}$ -aerogel. An approximate solution derived from the asymptotic solutions and perturbation theory is accurate to less than 0.6%. A key result of this work is the scaling function,  $F(T/T^*, \lambda_\kappa)$ , that describes the exact solution for the normalized thermal conductivity,  $\kappa/\kappa_{\text{el}}$ , for all pressures, temperatures (above  $T_c$ ) and aerogel density. A complete set of measurements of the thermal conductivity of  $^3\text{He}$ -aerogel for all  $T$ ,  $p$  and a wide range of aerogel  $mfp$  would provide a strong test of this theory, particularly the predicted scaling behavior based on two-channel scattering and the assumption of homogeneous disorder described by a single  $mfp$ . Conversely, systematic deviations from the predicted scaling function behavior should provide a quantitative measure of the role of fractal correlations associated with the structure of the aerogel. The limited data that is available already hints that two-channel scattering is insufficient and that spin-exchange scattering between itinerant  $^3\text{He}$  spins and localized  $^3\text{He}$  spins contributes to the low-temperature thermal conductivity.

### Acknowledgements

This work was supported in part by National Science Foundation Grant DMR-0805277 (JAS) and the Leverhulme Trust of the United Kingdom (PS).

### V. APPENDIX: $^3\text{He}$ SCATTERING AMPLITUDE

The binary collision amplitude for quasiparticles in pure  $^3\text{He}$  in the low-energy region near the Fermi surface depends on the momenta and the spin state of the initial and final pair of excitations. In particular the dimensionless scattering amplitude is

$$T_{\alpha_1\alpha_2;\alpha_3\alpha_4}(\mathbf{p}_1, \mathbf{p}_2; \mathbf{p}_3, \mathbf{p}_4) = 2N_f \times$$

where  $\mathbf{t}$  is formally defined by the matrix elements of a transition operator between incoming (1,2) and outgoing (3,4) quasiparticles. For a Fermi liquid with only exchange interactions such as  $^3\text{He}$  the total spin  $S$  and any one component,  $S_z$ , are conserved by collisions. For an unpolarized Fermi liquid there is no preferred direction for the spins to align. As a result all three spin-triplet amplitudes are equal and there are only two independent amplitudes corresponding to

the total spin  $S = 0$  and  $S = 1$ , which we label as the singlet ( $s$ ) and triplet ( $t$ ) amplitudes,

$$\mathbf{T}_s = \frac{1}{2} [\mathbf{T}_{\uparrow\downarrow;\uparrow\downarrow} - \mathbf{T}_{\uparrow\downarrow;\downarrow\uparrow} - \mathbf{T}_{\downarrow\uparrow;\uparrow\downarrow} + \mathbf{T}_{\downarrow\uparrow;\downarrow\uparrow}] \quad (135)$$

$$\begin{aligned} \mathbf{T}_t &= \frac{1}{2} [\mathbf{T}_{\uparrow\downarrow;\uparrow\downarrow} + \mathbf{T}_{\uparrow\downarrow;\downarrow\uparrow} + \mathbf{T}_{\downarrow\uparrow;\uparrow\downarrow} + \mathbf{T}_{\downarrow\uparrow;\downarrow\uparrow}] \\ &= \mathbf{T}_{\uparrow\uparrow;\uparrow\uparrow} = \mathbf{T}_{\downarrow\downarrow;\downarrow\downarrow}. \end{aligned} \quad (136)$$

Also note that amplitudes which differ by inversion of all the spin projections are equal,

$$\mathbf{T}_{\uparrow\uparrow;\uparrow\uparrow} = \mathbf{T}_{\downarrow\downarrow;\downarrow\downarrow}, \quad \mathbf{T}_{\uparrow\downarrow;\uparrow\downarrow} = \mathbf{T}_{\downarrow\uparrow;\downarrow\uparrow}, \quad \mathbf{T}_{\uparrow\downarrow;\downarrow\uparrow} = \mathbf{T}_{\downarrow\uparrow;\uparrow\downarrow}. \quad (137)$$

Thus, we use a short-hand notation,

$$\mathbf{T}_{\uparrow\uparrow} \equiv \mathbf{T}_{\uparrow\uparrow;\uparrow\uparrow} = \mathbf{T}_{\downarrow\downarrow;\downarrow\downarrow} \quad (138)$$

$$\mathbf{T}_{\uparrow\downarrow} \equiv \mathbf{T}_{\uparrow\downarrow;\uparrow\downarrow} = \mathbf{T}_{\downarrow\uparrow;\downarrow\uparrow} \quad (139)$$

$$\tilde{\mathbf{T}}_{\uparrow\downarrow} \equiv \mathbf{T}_{\uparrow\downarrow;\downarrow\uparrow} = \mathbf{T}_{\downarrow\uparrow;\uparrow\downarrow}, \quad (140)$$

and express the spin-projection amplitudes in terms of the singlet and triplet amplitudes

$$\mathbf{T}_{\uparrow\uparrow} = \mathbf{T}_t \quad (141)$$

$$\mathbf{T}_{\uparrow\downarrow} = \frac{1}{2} (\mathbf{T}_t + \mathbf{T}_s) \quad (142)$$

$$\tilde{\mathbf{T}}_{\uparrow\downarrow} = \frac{1}{2} (\mathbf{T}_t - \mathbf{T}_s). \quad (143)$$

The T-matrix can then be expressed in terms of  $\mathbf{T}_{t,s}$  and the corresponding symmetric (triplet) and anti-symmetric (singlet) spin matrix elements,

$$\mathbf{T}_{\alpha_1\alpha_2;\alpha_3\alpha_4} = \mathbf{T}_t \Sigma_{\alpha_1\alpha_2;\alpha_3\alpha_4}^{(+)} + \mathbf{T}_s \Sigma_{\alpha_1\alpha_2;\alpha_3\alpha_4}^{(-)}, \quad (144)$$

where

$$\Sigma_{\alpha_1\alpha_2;\alpha_3\alpha_4}^{(\pm)} = \frac{1}{2} (\delta_{\alpha_1\alpha_3} \delta_{\alpha_2\alpha_4} \pm \delta_{\alpha_1\alpha_4} \delta_{\alpha_2\alpha_3}). \quad (145)$$

Since there are only two independent amplitudes it is often useful to use the *symmetric* and *anti-symmetric* amplitudes defined as

$$\mathbf{T}^s = \frac{1}{2} (\mathbf{T}_{\uparrow\uparrow} + \mathbf{T}_{\uparrow\downarrow}) = \frac{1}{4} (3\mathbf{T}_t + \mathbf{T}_s) \quad (146)$$

$$\mathbf{T}^a = \frac{1}{2} (\mathbf{T}_{\uparrow\uparrow} - \mathbf{T}_{\uparrow\downarrow}) = \frac{1}{4} (\mathbf{T}_t - \mathbf{T}_s). \quad (147)$$

Inverting, we have

$$\mathbf{T}_t = (\mathbf{T}^s + \mathbf{T}^a) \quad (148)$$

$$\mathbf{T}_s = (\mathbf{T}^s - 3\mathbf{T}^a). \quad (149)$$

The two sets of amplitudes,  $\mathbf{T}^{s,a}$  or  $\mathbf{T}_{t,s}$ , define different, but equivalent representations for the spin-dependent T matrix. The  $\mathbf{T}^{s,a}$  amplitudes are the amplitudes for the T-matrix expressed in terms of the direct "particle-hole" channel,  $1 \rightarrow 3$  and  $2 \rightarrow 4$ ,

$$\mathbf{T}_{\alpha_1\alpha_2;\alpha_3\alpha_4} = \mathbf{T}^s \delta_{\alpha_1\alpha_3} \delta_{\alpha_2\alpha_4} + \mathbf{T}^a \boldsymbol{\sigma}_{\alpha_1\alpha_3} \cdot \boldsymbol{\sigma}_{\alpha_2\alpha_4}. \quad (150)$$

For quasiparticle scattering on the Fermi surface the scattering amplitudes,  $\mathbf{T}_{t,s}$ , reduce to functions of the *directions* of the quasiparticle momenta on the Fermi surface,

$$\mathbf{T}_{t,s}(\mathbf{p}_1, \mathbf{p}_2; \mathbf{p}_3, \mathbf{p}_4) \rightsquigarrow \mathbf{T}_{t,s}(\hat{\mathbf{p}}_1, \hat{\mathbf{p}}_2; \hat{\mathbf{p}}_3, \hat{\mathbf{p}}_4). \quad (151)$$

Furthermore, rotational invariance implies that  $\mathbf{T}_{t,s}$  can be expressed in terms of the *relative* direction cosines,

$$x_2 = \hat{\mathbf{p}}_2 \cdot \hat{\mathbf{p}}_1 \equiv \cos \theta = \hat{\mathbf{p}}_3 \cdot \hat{\mathbf{p}}_4, \quad (152)$$

$$x_3 = \hat{\mathbf{p}}_3 \cdot \hat{\mathbf{p}}_1 = \cos \theta_3 = \hat{\mathbf{p}}_4 \cdot \hat{\mathbf{p}}_2, \quad (153)$$

$$x_4 = \hat{\mathbf{p}}_4 \cdot \hat{\mathbf{p}}_1 = \cos \theta_4 = \hat{\mathbf{p}}_3 \cdot \hat{\mathbf{p}}_3. \quad (154)$$

The fourth column of equalities follows from momentum conservation for  $|\mathbf{p}_i| = p_f$ ,

$$\hat{\mathbf{p}}_1 + \hat{\mathbf{p}}_2 = \hat{\mathbf{p}}_3 + \hat{\mathbf{p}}_4. \quad (155)$$

The conservation law also implies that there are only *two* independent angles. We adopt Abrikosov and Khalatnikov's parametrization<sup>4</sup> in terms of the angle  $\theta$  between the two incoming momenta, and  $\phi$ , the angle between the planes defined by  $\mathbf{n} = \hat{\mathbf{p}}_1 \times \hat{\mathbf{p}}_2$  and  $\mathbf{n}' = \hat{\mathbf{p}}_3 \times \hat{\mathbf{p}}_4$ ,

$$\cos \phi = \frac{\mathbf{n} \cdot \mathbf{n}'}{|\mathbf{n}| |\mathbf{n}'|} = \frac{x_3 - x_4}{1 - x_2}. \quad (156)$$

Thus,  $\mathbf{T}_{t,s}(\hat{\mathbf{p}}_1, \hat{\mathbf{p}}_2; \hat{\mathbf{p}}_3, \hat{\mathbf{p}}_4) = \mathbf{T}_{t,s}(\theta, \phi)$ .

The Pauli exclusion principle requires the T-matrix to be anti-symmetric under exchange of either the initial or the final state of the two fermions. Thus, the spin-singlet (triplet) amplitude is necessarily symmetric (anti-symmetric) under exchange of the initial or final momenta, or in terms of the scattering angle,

$$\mathbf{T}_s(\theta, \phi + \pi) = +\mathbf{T}_s(\theta, \phi) \quad (157)$$

$$\mathbf{T}_t(\theta, \phi + \pi) = -\mathbf{T}_t(\theta, \phi). \quad (158)$$

Thus, we can formally expand the singlet (triplet) amplitudes as a sum over even (odd) functions of  $\cos(m\phi)$ ,

$$\mathbf{T}_s(\theta, \phi) = \sum_{m=0}^{\text{even}} A_s^{(m)}(\cos \theta) \cos(m\phi), \quad (159)$$

$$\mathbf{T}_t(\theta, \phi) = \sum_{m=1}^{\text{odd}} A_t^{(m)}(\cos \theta) \cos(m\phi). \quad (160)$$

Note that  $\mathbf{T}_t$  vanishes for  $\phi = \pi/2$  and  $\phi = 3\pi/2$ . For these angles the momentum transfer in the direct and exchange channels is identical, in which case exchange symmetry requires the triplet amplitude to vanish identically.

Microscopic analysis of the two-particle propagator and its relation to the quasiparticle scattering amplitude leads to an identity between the scattering amplitude in the forward direction, and the Landau parameters,  $F_\ell^{s,a}$ , that define the quasiparticle molecular fields. In terms of the symmetric and anti-symmetric amplitudes in the p-h channel, Landau's identity for the forward scattering amplitude is<sup>23</sup>,

$$\mathbf{T}^{s,a}(\theta, \phi = 0) = \sum_{\ell=0}^{\infty} A_\ell^{s,a} \mathcal{P}_\ell(\cos \theta), \quad (161)$$

where

$$A_\ell^{s,a} = \frac{F_\ell^{s,a}}{1 + F_\ell^{s,a}/(2\ell + 1)}. \quad (162)$$

In terms of the singlet and triplet amplitudes for  $\phi = 0$ ,

$$\mathbf{T}_s(\theta, \phi = 0) = \sum_{\ell \geq 0} (A_\ell^s - 3A_\ell^a) \mathcal{P}_\ell(\cos \theta) \quad (163)$$

$$\mathbf{T}_t(\theta, \phi = 0) = \sum_{\ell \geq 0} (A_\ell^s + A_\ell^a) \mathcal{P}_\ell(\cos \theta). \quad (164)$$

Exchange symmetry leads to an additional constraint on the triplet amplitude. In the limit  $\theta = 0$ ,  $\phi = 0$ , i.e. for  $\hat{\mathbf{p}}_1 = \hat{\mathbf{p}}_2 = \hat{\mathbf{p}}_3 = \hat{\mathbf{p}}_4$ , the triplet amplitude necessarily vanishes. Thus, from Eq. (164) we obtain the forward scattering sum rule (FSSR),

$$\lim_{\theta \rightarrow 0} \mathbf{T}_t(\theta, 0) = \sum_{\ell \geq 0} (A_\ell^s + A_\ell^a) \equiv 0. \quad (165)$$

### *s-p-d Scattering*

Several microscopic and phenomenological theories have been proposed for the quasiparticle scattering amplitude in  $^3\text{He}$ .<sup>13,24,26,33</sup> Here we adopt a slightly modified version of the model proposed by Dy and Pethick.<sup>13</sup> They proposed a minimal model for the scattering amplitude that obeys exchange anti-symmetry. In particular, if we assume the singlet and triplet scattering amplitudes are to a good approximation given by the  $m = 0$  and  $m = 1$  terms, we have  $\mathbf{T}_s \simeq A_s(\cos \theta)$  and  $\mathbf{T}_t \simeq A_t(\cos \theta) \cos \phi$ . In this case we can fix the expansion coefficients of  $A_{t,s}(\cos \theta)$  in terms of the forward-scattering amplitudes,  $A_\ell^{s,a}$ , and thus the Landau parameters,  $F_\ell^{s,a}$ ,<sup>13</sup>

$$\mathbf{T}_s \simeq \sum_{\ell \geq 0} (A_\ell^s - 3A_\ell^a) \mathcal{P}_\ell(\cos \theta), \quad (166)$$

$$\mathbf{T}_t \simeq \sum_{\ell \geq 0} (A_\ell^s + A_\ell^a) \mathcal{P}_\ell(\cos \theta) \cos \phi. \quad (167)$$

The quasiparticle lifetime,  $\tau_{\text{in}}(T)$  in Eq. 1, as well as the thermal transport time,  $\tau_\kappa(T)$ , due to binary quasiparticle collisions in pure  $^3\text{He}$  are determined by angular averages of the spin-averaged transition probability,

$$\frac{1}{\tau_{\text{in}}} = \frac{N_f^2}{v_f p_f} \langle W \rangle (k_B T)^2 \quad (168)$$

$$\tau_\kappa = S_\kappa^\infty(\lambda_\kappa) \tau_{\text{in}}, \quad (169)$$

with

$$\lambda_\kappa \equiv \langle W (1 + 2 \cos \theta) \rangle / \langle W \rangle, \quad (170)$$

where  $W = \frac{1}{4}W_{\uparrow\uparrow} + \frac{1}{2}W_{\uparrow\downarrow}$  and the angular average is defined in Eq. 51. Writing  $W_{ab} = \frac{\pi}{2}\hbar^{-1}N_f^{-2}\bar{W}_{ab}$ , the transition

probability can be expressed in terms of the dimensionless singlet and triplet scattering amplitudes,

$$\bar{W} = |\mathbf{T}_s|^2 + 3|\mathbf{T}_t|^2 + 2\Re\{\mathbf{T}_t\mathbf{T}_s^*\}, \quad (171)$$

and the quasiparticle lifetime becomes,

$$\frac{1}{\tau_{\text{in}}} = \frac{\pi}{32} \hbar^{-1} \frac{(k_B T)^2}{E_f} \langle \bar{W} \rangle. \quad (172)$$

Note that for weighted averages of  $\bar{W}$  in which the weight function is even under exchange (i.e.  $\phi \rightarrow \phi + \pi$ ) the cross term in Eq. (171) vanishes. Similarly, for the thermal transport time we can write  $\lambda_\kappa = \Lambda_\kappa / \langle \bar{W} \rangle$  where

$$\Lambda_\kappa = \langle (1 + 2 \cos \theta) \bar{W} \rangle. \quad (173)$$

In the *spd* model the Fermi-surface average of the rate becomes,

$$\langle \bar{W} \rangle = \langle A_s^2 \rangle + \frac{3}{2} \langle A_t^2 \rangle, \quad (174)$$

We evaluate this rate in terms of Legendre expansion of the forward-scattering amplitudes. For either singlet or triplet channel,

$$A(\cos \theta) = \sum_\ell A_\ell \mathcal{P}_\ell(\cos \theta). \quad (175)$$

The angular average of  $A^2$  is given by

$$\langle A^2 \rangle = \sum_{\ell\ell'} C_{\ell\ell'} A_\ell A_{\ell'}, \quad (176)$$

where

$$C_{\ell\ell'} \equiv \int_0^1 dx \mathcal{P}_\ell(2x^2 - 1) \mathcal{P}_{\ell'}(2x^2 - 1). \quad (177)$$

Similarly, for the angular averages of the form,

$$\langle A^2 (1 + 2 \cos \theta) \rangle = \sum_{\ell\ell'} L_{\ell\ell'} A_\ell A_{\ell'}, \quad (178)$$

with

$$L_{\ell\ell'} \equiv \int_0^1 dx (4x^2 - 1) \mathcal{P}_\ell(2x^2 - 1) \mathcal{P}_{\ell'}(2x^2 - 1). \quad (179)$$

These coefficients are listed in Table I for  $\ell, \ell' \leq 2$ .

The input for our calculations of the transport properties of bulk  $^3\text{He}$  as well as  $^3\text{He}$ -aerogel are the Fermi-liquid parameters. The measured values of these parameters are collected in Ref. 19, and are also available online.<sup>17</sup> The Landau interaction parameters,  $F_0^s$ ,  $F_1^s$ , and  $F_0^a$  are accurately known from measurements of the heat capacity, first-sound velocity and magnetic susceptibility of pure normal  $^3\text{He}$ , while determinations of  $F_2^s$  and  $F_1^a$  have also been obtained from



$C_{\ell\ell'}$	0	1	2
0	1	-1/3	1/5
1	-1/3	7/15	-23/105
2	1/5	-23/105	11/105

$L_{\ell\ell'}$	0	1	2
0	1/3	3/5	-5/21
1	3/5	-1/21	1/3
2	-5/21	1/3	-71/1155

TABLE I: Coefficients defining the angular averages of  $\langle \bar{W} \rangle$  ( $C_{\ell\ell'}$ ) and  $\langle \bar{W}(1 + 2 \cos \theta) \rangle$  ( $L_{\ell\ell'}$ ) in the *spd* scattering model.

measurements of the zero sound velocity and spin-wave resonance for normal  $^3\text{He}$ , respectively. However, these parameters are not as accurately determined. Less is known about the magnitude and pressure dependence of the  $\ell = 2$  contribution to the exchange interaction,  $F_2^a$ ,<sup>14</sup> and much less is known quantitatively about the Landau interaction parameters corresponding to harmonics  $\ell > 2$ , although evidence of interactions in higher order scattering channels is suggested by the observation of high frequency pair exciton<sup>32</sup> modes in superfluid  $^3\text{He-B}$ .<sup>12</sup>

The scattering model we use throughout is defined by Eqs. (166) and (167) with the added assumption that we truncate the expansion, i.e. set  $A_\ell^{s,a} = 0$  for  $\ell \geq 3$ . This approximation is reasonable if the contributions to the Fermi-surface averages of the scattering rate fall off sufficiently rapidly with increasing  $\ell > 2$ .

The *spd* model with the Fermi liquid data for  $\ell \leq 2$  as input qualitatively describes the decrease in the transport time,  $\tau_\kappa T^2$ , with increasing pressure (shown in Fig. 2) and is within 25% of the experimental values for  $\tau_\kappa T^2$  over the full pressure range. However, the comparison clearly shows that

the *spd* model, or the accuracy of the known Fermi liquid data is inadequate, or both. The most problematic aspect of the *spd* model as it stands is that the FSSR is badly violated, when evaluated with  $A_\ell^{s,a} = 0$  for  $\ell \geq 3$ . In particular the largest violation in the FSSR,

$$S_{\text{error}} = \sum_{\ell} (A_\ell^s + A_\ell^a) \approx -1.0, \quad (180)$$

is at low pressures, which is also where the discrepancy (refer to Fig. 2) between theory (solid line) and experiment (red diamonds) is greatest. This is a significant violation of the Pauli exclusion principle, and is an indication that either the determinations of  $F_{1,2}^a$  are inaccurate, that there is significant weight in the interaction channels for  $\ell \geq 3$ , or both.

Respecting the Pauli exclusion principle, by enforcing the FSSR, is likely more important than knowing precisely the distribution of higher angular momentum channels that account for the missing weight in Eq. 180. Thus, we enforce the FSSR by fixing the least known material parameter in the *spd* model, i.e. we replace

$$A_2^a \rightarrow A_2^{a'} = A_2^a - S_{\text{error}}. \quad (181)$$

The importance of enforcing the FSSR appears to be born out by the improvement between theory (black dots) and experiment shown in Fig. 2. For pressures below  $p \leq 25$  bar the agreement is nearly perfect. Thus, the deviations between theory and experiment at higher pressures likely reflects real limitations of the *spd* model, i.e. there is scattering that reduces heat transport that is outside the *spd* scattering model.

- 
- <sup>1</sup> W.R. Abel, R.T. Johnson, J.C. Wheatley, and W. Zimmerman. *Phys. Rev. Lett.*, 18(18):737–740, Jan 1967.
- <sup>2</sup> M. Abramowitz and I.A. Stegun. *Handbook of Mathematical Functions*. U.S. Government Printing Office, Washington D.C., tenth printing edition, 1972.
- <sup>3</sup> A. A. Abrikosov. *Fundamentals of the Theory of Metals*. North-Holland, Amsterdam, 1988.
- <sup>4</sup> A. A. Abrikosov and I. Khalatnikov. *Sov. Phys. Uspeki*, 66:68, 1958.
- <sup>5</sup> A.A. Abrikosov. *Sov. Phys. JETP*, 5:1174, 1957.
- <sup>6</sup> G. Baramidze and G. Kharadze. *Physica*, 284, 2000.
- <sup>7</sup> B. I. Barker, L. Polukhina, J. F. Poco, L. W. Hrubesh, and D. D. Osheroff. *J. Low Temp. Phys.*, 113:635, 1998.
- <sup>8</sup> G. Baym and C. J. Pethick. *The Physics of Solid and Liquid Helium, Part 2*, pages 1–122. Wiley, New York, 1978.
- <sup>9</sup> G. Baym and C. J. Pethick. *Landau Fermi-Liquid Theory*. Wiley, New York, 1991.
- <sup>10</sup> Alan J Bennett and M J Rice. *Phys. Rev.*, 185(3):968–970, 1969.
- <sup>11</sup> G. A. Brooker and J. Sykes. *Phys. Rev. Lett.*, 21:279, 1968.
- <sup>12</sup> J P Davis, J P Davis, J Pollanen, J Pollanen, H Choi, H Choi, J A Sauls, J A Sauls, W P Halperin, and W P Halperin. *Nature Physics*, 4(7):571, Apr 2008.
- <sup>13</sup> K. S. Dy and C. J. Pethick. *Phys. Rev.*, 185(1):373–384, Sep 1969.
- <sup>14</sup> R. S. Fishman and J. A. Sauls. *Phys. Rev. B*, 33:6068, 1986.
- <sup>15</sup> J. Fricke. *Aerogels*. Springer-Verlag, Berlin, 1986.
- <sup>16</sup> Dennis S Greywall. *Phys. Rev. B*, 29(9):4933–4945, May 1984.
- <sup>17</sup> T. Haard. Helium-Three Calculator, 2000, url: <http://spindry.phys.northwestern.edu/he3.htm>.
- <sup>18</sup> W. P. Halperin and J. A. Sauls. *arXiv*, cond-mat.supr-con:0408593, Jan 2004. 10 pages with 12 figures.
- <sup>19</sup> W. P. Halperin and E. Varoquaux. In W. P. Halperin and L. P. Pitaevskii, editors, *Helium Three*, page 353. Elsevier Science Publishers, Amsterdam, 1990.
- <sup>20</sup> H. Højgaard-Jensen, H. Smith, and J. W. Wilkins. *Phys. Lett.*, 27A:532, 1968.
- <sup>21</sup> L. D. Landau. *Sov. Phys. JETP*, 30:1058, 1956.
- <sup>22</sup> L. D. Landau. *Sov. Phys. JETP*, 32:59, 1957.
- <sup>23</sup> L. D. Landau. *Sov. Phys. JETP*, 35:70, 1959.
- <sup>24</sup> K. Levin and O. T. Valls. *Phys. Rep.*, 98:1, 1983.
- <sup>25</sup> R. Nomura, G. Gervais, T. M. Haard, N. Mulders, and W. P. Halperin. *Phys. Rev. Lett.*, 85:4325, 2000.
- <sup>26</sup> M Pfitzner and P Wölfle. *J Low Temp Phys*, 51(5-6):535–559, Dec 1983.
- <sup>27</sup> J. V. Porto and J. M. Parpia. *Phys. Rev. B*, 59(22):14583–14592, 1999.
- <sup>28</sup> J.V. Porto and J.M. Parpia. *Phys. Rev. Lett.*, 74:4667, 1995.

- <sup>29</sup> D. Rainer and J. A. Sauls. *J. Low Temp. Phys.*, 110:525, 1998. Proceedings of *QFS97, Paris*.
- <sup>30</sup> P. A. Reeves, G. Tvalashvili, S. N. Fisher, A. M. Guénault, and G. R. Pickett. *J. Low Temp. Phys.*, 129:185, 2002.
- <sup>31</sup> J. A. Sauls, Yu. M. Bunkov, E. Collin, H. Godfrin, and P. Sharma. *Phys. Rev. B*, 72(2):024507, 2005.
- <sup>32</sup> J. A. Sauls and J. W. Serene. *Phys. Rev. B*, 23:4798, 1981.
- <sup>33</sup> J. A. Sauls and J. W. Serene. *Phys. Rev.*, B24:183, 1981.
- <sup>34</sup> J. A. Sauls and P. Sharma. *Phys. Rev. B*, 68:224502, 2003.
- <sup>35</sup> H. Smith and H. Højgaard-Jensen. *Transport Phenomena*. Clarendon Press, Oxford, 1989.
- <sup>36</sup> D.T. Sprague, T.M. Haard, J.B. Kycia, M. Rand, Y. Lee, P.J. Hamot, and W.P. Halperin. *Physical Review Letters*, 75(4):661–664, Jan 1995.
- <sup>37</sup> J. Sykes and G. A. Brooker. *Annals of Physics*, 56(1):1–39, Jan 1970.
- <sup>38</sup> E. V. Thuneberg, S.-K. Yip, M. Fogelström, and J. A. Sauls. *Phys. Rev. Lett.*, 80:2861, 1998.
- <sup>39</sup> P Venkataramani and J. A. Sauls. *Physica B*, 284:297–298, Dec 2000.
- <sup>40</sup> This is not entirely true as relatively weak interactions between quasiparticles with zero total momentum on the Fermi surface eventually leads to the Cooper instability and to superfluidity at low temperatures,  $k_B T_c \lll E_f$ .
- <sup>41</sup> For 98% aerogel this implies  $T \gtrsim 1$  mK.